On Li-bearing micas: estimating Li from electron microprobe analyses and an improved diagram for graphical representation

GERHARD TISCHENDORF
Neumannstr. 106, 13189 Berlin, Germany
BÄRBEL GOTTESMANN, HANS-JÜRGEN FÖRSTER, AND ROBERT B. TRUMBULL
GeoForschungsZentrum Potsdam, Dept. 4.2, Telegrafenberg A50, 14473 Potsdam, Germany

Abstract

Lithium may constitute an essential element in micas, yet it cannot be detected by the electron microprobe. Since Li is critical for correctly classifying micas and properly calculating their formulae, several methods have been proposed to overcome this analytical deficiency. We offer empirical relationships between Li_2O and SiO_2, MgO, F, and Rb in trioctahedral micas, and between Li_2O and F as well as Rb in dioctahedral micas. The resultant regression equations enable lithium contents to be sufficiently well estimated from EPM analyses within the range of validity discussed.

Secondly, we introduce an easy to handle, new diagram with the axis variables [Mg−Li] and $[Fe_{tot} + Mn + Ti - Al^{VI}]$ for graphical representation and discuss its scientific rationale. Being based on absolute abundances of cations in the octahedral layer, the diagram provides a simple means to classify micas in terms of composition and octahedral site occupancy, and it also allows compositional relationships between Li-bearing and Li-free mica varieties as well as between trioctahedral and dioctahedral micas to be displayed on a single, two-dimensional diagram.

KEYWORDS: mica, lithium, correlation, classification, electron microprobe.

Introduction

THE importance of micas for petrologic or metallogenetic studies of metamorphic and igneous rocks is well established and has been the subject of a great deal of research (see Bailey, 1984, for an overview). The reason for their popularity is that micas form one of the most common mineral groups, stable over a wide range of pressure and temperature in rocks of many kinds. They have a highly variable chemical composition and the ability to exchange components readily with fluids or solid phases as external conditions change. Being hydrous phases, micas are sensitive to the fugacities of water, oxygen, fluorine and other volatile species. The micas, therefore, are useful as monitors of the physico-chemical environment in which they grew. This aspect is particularly important in the case of granites, in many of which micas are the only mafic and hydrous phases present.

This paper is concerned with Li-bearing micas because of their importance in evolved granites and related pegmatites and aplites. The basis of the work is a compilation of several hundred Li-mica analyses, many from sources in the literature and many others from published and unpublished data sets of our own. Most of the latter represent micas from the Erzgebirge province, hosted in Variscan granites, or in a few cases from associated pegmatites as well as from greisens in tin deposits. Analyses of mica from metamorphic rocks of the Erzgebirge and of nearby granodioritic and granitic complexes of Cadomian and Variscan ages are also represented in the data compilation (Fig. 1).

Our objective is twofold. Firstly, we expand on the works of Stone *et al.* (1988) and Tindle and Webb (1990), and explore ways to indirectly estimate Li concentrations in both trioctahedral and dioctahedral micas from electron microprobe analyses by empirical approaches based on element correlations. Secondly, we introduce a new diagram with the axis

Mineralogical Magazine, December 1997, Vol. 61, pp. 809–834

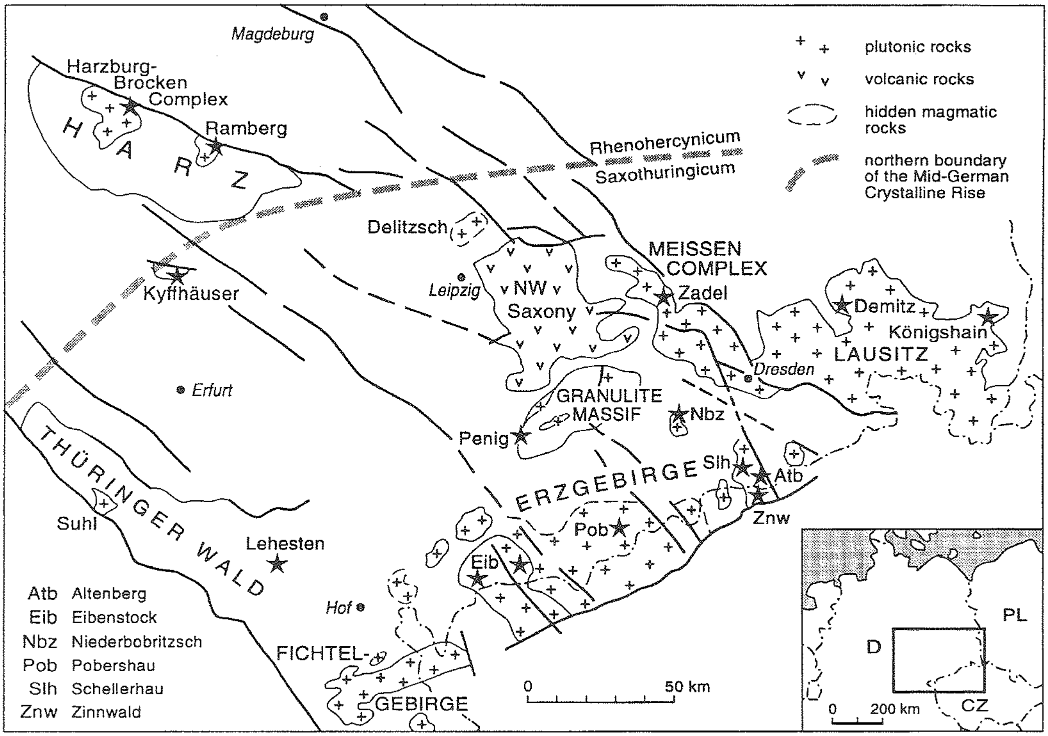

FIG. 1. Simplified geological sketch map showing the sample localities of trioctahedral micas listed in Table 1.

variables [Mg−Li] and [Fe_{tot} + Mn + Ti−Al^{VI}], which provides a simple means to classify micas in terms of composition and octahedral site occupancy (trioctahedral and dioctahedral series), and which also allows the compositional relationships between Li-bearing and Li-free mica varieties to be displayed on a single, two-dimensional diagram.

Today, the vast majority of chemical analyses of mica composition for petrologic studies are performed *in situ* by electron microprobe. Bulk analysis of mineral separates can be misleading or non-representative because more than one generation of micas may be present in a given sample, and because individual mica grains are commonly zoned, especially in fractionated granites and related aplites (Fonteilles, 1987; Monier *et al.*, 1987; Hecht, 1993; Gottesmann *et al.*, 1994*a*; Charoy *et al.*, 1995). Intergrowths, overgrowths and inclusions of other minerals in mica are other factors which pose no great problem for the microprobe method but can seriously affect the results of bulk chemical analysis.

One disadvantage of electron microprobe analyses of micas is that ferric and ferrous iron cannot be distinguished. Micas are poorly suited for calculation of ferric and ferrous iron by stoichiometry because site vacancies are common, and because manganese can be present in the divalent and trivalent state. Therefore Fe^{2+} and Fe^{3+} must be treated together as Fe_{tot}. The inability of the microprobe to analyse lithium is a serious problem in evolved granites, aplites and pegmatites, where Li is an essential component in both dioctahedral and trioctahedral micas (Tischendorf *et al.*, 1969; Lapides *et al.*, 1977; Stone *et al.*, 1988). Failure to analyse Li in micas from this environment means a loss of important petrogenetic information as well as systematic errors in calculating structural formulae (Tindle and Webb, 1990). There are established methods of micro-analysis capable of analysing lithium, SIMS (Henderson *et al.*, 1989; Charoy *et al.*, 1995) and laser-ablation ICP-MS (Bea *et al.*, 1994), but they are expensive and out of reach for most researchers; thus they do not represent practical alternatives to the electron microprobe at present.

Fortunately, it turns out that lithium correlates strongly with several other elements in micas which can be measured routinely by electron microprobe, and this offers a way to estimate Li contents from a microprobe analysis. Tindle and Webb (1990) utilized this in a study of element correlations in Li micas from a literature compilation, and they suggested the following equation to estimate Li from the Si content: $Li_2O = (0.287 \times SiO_2) - 9.552$. These authors limit application of their equation to trioctahedral micas with less than 8 wt.% MgO. In this paper we take the same approach and examine element correlations in both trioctahedral and dioctahedral lithian micas separately, making a particular effort to find workable solutions for the cases which Tindle and Webb (1990) found problematical, namely, the Mg-rich trioctahedral and the dioctahedral micas.

Mica compositions and covariances with lithium

Trioctahedral micas. The most frequently applied nomenclature for trioctahedral micas was introduced by Foster (1960*a,b*), and is based on the octahedral site occupancy. Li-bearing micas are represented in a triangular diagram with the corner variables Li; R^{2+} (Fe^{2+}, Mn^{2+}, Mg); and octahedral R^{3+} (Al, Fe^{3+}) + Ti^{4+} (Fig. 2).

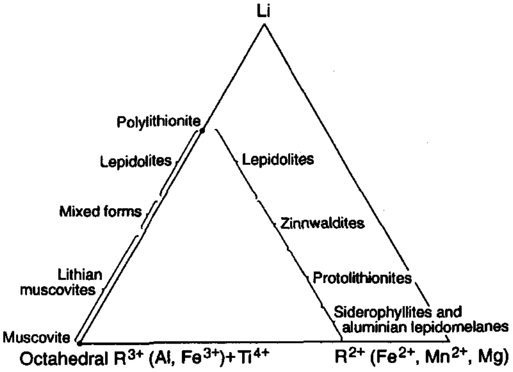

FIG. 2. Relationship between Li and octahedral cations R^{2+} (Fe^{2+}, Mn^{2+}, Mg) and R^{3+} (Al^{IV}, Fe^{3+}) + Ti^{4+} (according to Foster, 1960*b*).

We examine below the correlations of Li_2O with other elements in the octahedral layer (TiO_2, Al_2O_3, FeO_{tot}, MnO, MgO) as well as with SiO_2, F, and Rb_2O. As recognized by Tindle and Webb (1990), SiO_2 alone does not permit estimation of lithium over the entire range of mica compositions. Thus we focussed on the search for elements alternative or supplementary to silica. The data used were taken from our own analyses and from the literature which met the following criteria: (a) Li was determined, (b) the analyses are commonly not older than 25 years (to ensure comparable data quality), and (c) compositions of concentrates appeared to represent pure trioctahedral compositions not contaminated by dioctahedral micas.

Figures 3–6 plot analyses of trioctahedral micas (screened by the above criteria a–c) which were taken from the literature, our own published data (Tischendorf *et al.*, 1969, *n* = 66; Gottesmann *et al.*, 1994*b*, *n* = 4) and about 100 unpublished analyses (see Appendix). Several representative analyses from the unpublished data are given in Table 1 (see Fig. 1 for sample localities). Details on the petrology and geochemistry of the rocks from which the micas were separated are given by Tischendorf *et al.* (1987) and Förster and Tischendorf (1996).

Figures 3*a–c* show the main compositional features of the micas. They form three compositional series, labelled on the figures as: Mg–Fe series (phlogopite, Mg-biotite, Fe-biotite, siderophyllite, lepidomelane), Li–Fe series (Li-bearing siderophyllite, protolithionite) and Li–Al series (zinnwaldite, lepidolite). The SiO_2 and Al_2O_3 variation (Fig. 3*a*) is large and irregular, with a weak negative correlation and considerable overlap among the three compositional series which is partly caused by the presence of Al^{IV} and Al^{VI}. The Li–Al series shows the greatest range in composition, with Al_2O_3 contents from less than 15 wt.% (Bargar *et al.*, 1973; Skosyreva and Vlasova, 1983; Uhlig, 1992) to over 25 wt.% (Heinrich, 1967). Total iron–silica distributions (Fig. 3*b*) are more regular than alumina–silica, but there is complete overlap of the Mg-biotite–Fe-biotite and siderophyllite varieties. The diagram of MgO and SiO_2 (Fig. 3*c*) shows the most regular variation and good discrimination among the three mica series, which has been recognized before by other workers (e.g. Tindle and Webb, 1990). Note that we use a logarithmic scale for MgO to better illustrate the correlation with SiO_2 over the extreme compositional range of MgO. The important feature of this diagram is that the correlation between MgO and SiO_2 is negative in the Li–Fe and Li–Al series (< 6 wt.% MgO), and positive in the Mg–Fe series. This transition in behaviour has an effect on the Li distribution in the low-Mg and high-Mg micas, and must be born in mind when one considers the correlations of Li with Mg and Si (see below).

The variation of Li_2O with other chemical components of trioctahedral micas is examined in Fig. 4*a–f*. In most of these, there are ranges of composition with different degrees of correlation or even reverses in the sense of correlation. Table 2 lists regression equations describing what we found to be the best chemical correlations, and the range of compositions for which they are valid. The excellent positive correlation of SiO_2 and Li_2O (Fig. 4*a*) was already noted and used by Tindle and Webb (1990) for calculating Li from a regression equation. The

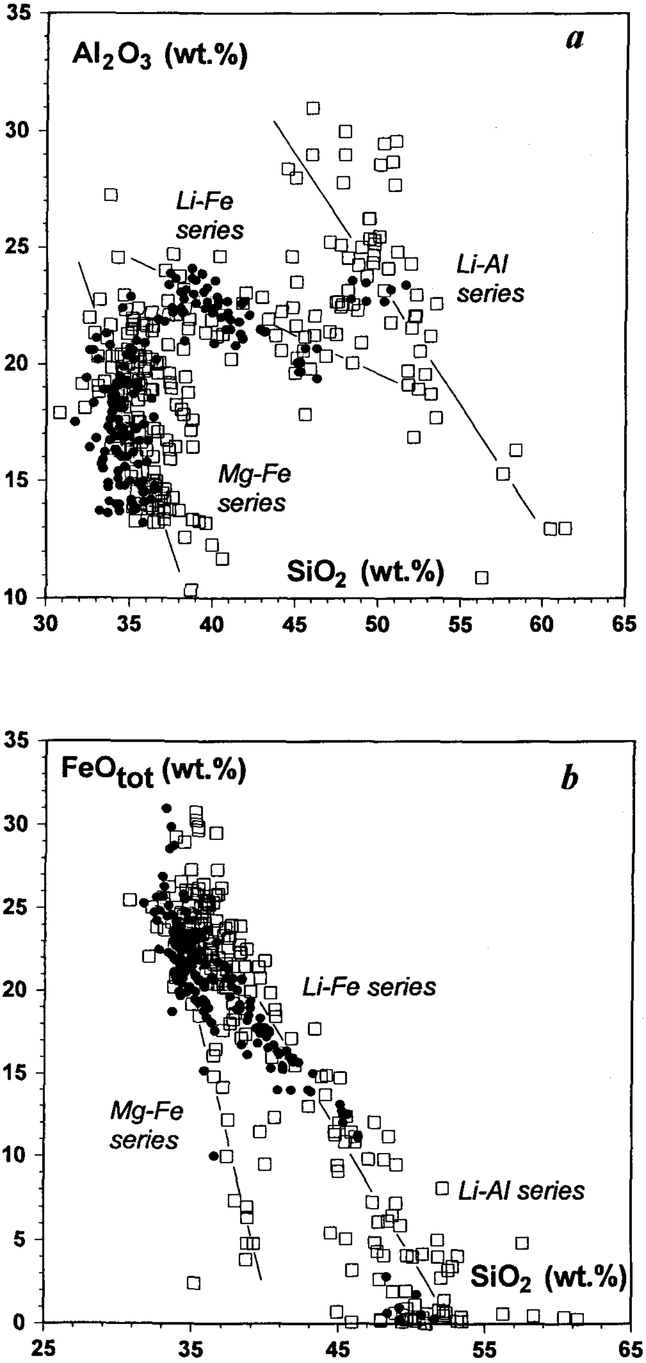
a
Al2O3 (wt.%)
Li-Fe series
Li-Al series
Mg-Fe series
SiO2 (wt.%)
10
15
20
25
30
35
30
35
40
45
50
55
60
65
b
FeOtot (wt.%)
Li-Fe series
Mg-Fe series
Li-Al series
SiO2 (wt.%)
0
5
10
15
20
25
30
35
25
35
45
55
65

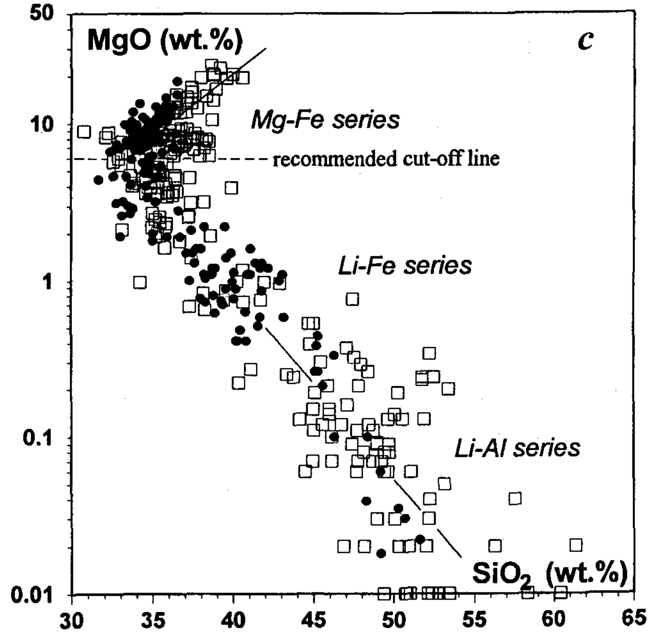

FIG. 3*a*–*c*. Variation of SiO_2 with Al_2O_3 (*a*), FeO_{tot} (*b*), and MgO (*c*) in trioctahedral micas. Dots mark analyses from the authors (n = 169), open squares mark analyses from the literature (n = 262 – 265).

figure demonstrates that this approach can only work for micas with Li_2O values greater than about 0.6 wt.%. For micas with less lithium, the positive correlation breaks down and turns negative in the concentration range below about 0.5 wt.% (corresponding to approximately 35 wt.% SiO_2 or 6 wt.% MgO). In terms of MgO concentration (see discussion below), a workable value for the cut-off is 6 wt.%. Using this value, our data in the range of MgO < 6 wt.% yields an essentially identical regression equation as the previous authors:

$$Li_2O = (0.289SiO_2) - 9.658 \quad (R^2 = 0.912, n = 232) \quad [tri\ 1]$$

Formally, this equation is valid only down to a SiO_2 value of 33.4 wt.%, where it cuts the abscissa. In practice, we recommend application of this equation to micas with SiO_2 exceeding 34 wt.%. Micas with lower values of SiO_2, of course, contain some finite amount of lithium.

The variations of Li_2O with Al_2O_3 and with MnO (Figs. 4*b*–*c*) are quite irregular, particularly in the case of MnO, and therefore of no value for predicting Li contents from microprobe analyses. Li_2O and Al_2O_3 are positively correlated for members of the Mg–Fe and Li–Fe series. In contrast, for micas of the Li–Al series two different trends are apparent. Within the Li–Al series, micas relatively poor in Li are rich in Al, whereas those strongly enriched in Li are depleted in both Al^{VI} and Al^{IV}.

The variation of Li_2O with total Fe is shown in Fig. 4*d*, and this is a further excellent illustration of the switch in sense and degree of correlation with changing Li concentration (cf. Fig. 4*a*). Above about 0.8 wt.% Li_2O there is a very good negative correlation of total iron and lithium; at values between 0.8 and 0.2 wt.% there is virtually no correlation, and below 0.2% a positive correlation is observed. We have examined the correlations of Li_2O with FeO and Fe_2O_3 separately (not shown) and found that the diagrams are similar to that of Fig. 4*a* but show more scatter. Furthermore, of course, microprobe analyses must be cast in terms of total iron and so the separate relationships of lithium with ferric and ferrous iron are of no significance to the question at hand.

Titanium and magnesium both show a steady inverse correlation with lithium (Figs. 4*e*–*f*). In the TiO_2–Li_2O diagram this correlation breaks down below about 0.1 wt.% Li_2O. In the case of MgO, curve-fitting leads to the following expression which is valid for the full range of mica compositions:

$$Li_2O = [2.7/(0.35 + MgO)] - 0.13 \quad (R^2 = 0.880, n = 434) \quad [tri\ 2]$$

TABLE 1. Chemical analyses of mica separates from various occurrences in eastern Germany

Region	Thüringer Wald	Meissen complex	Erzgebirge	Lausitz	Kyffhäuser	Harz	Lausitz	Harz
Locality	Lehesten	Zadel	Niederbobritzsch	Demitz	Bärenköpfe	Brocken	Königshain	Ramberg
Rock type	kersantite	granodiorite	monzogranite	granodiorite	granodiorite	monzogranite	monzogranite	two-mica syenogranite
Sample	312	128	98	503	650	906	520	901
SiO_2	37.1	36.5	34.1	35.0	33.3	34.1	33.5	33.6
TiO_2	2.9	2.9	3.9	3.5	3.9	3.2	2.9	2.4
Al_2O_3	14.8	15.4	14.8	16.8	16.8	13.8	13.9	20.8
Fe_2O_3	1.47	2.0	2.95	1.82	2.79	2.53	3.68	1.80
FeO	8.29	15.5	19.22	19.91	21.28	26.5	27.72	24.90
MnO	0.11	0.83	0.46	0.30	0.56	0.54	0.65	0.8
MgO	18.5	12.2	10.3	8.1	6.9	4.3	3.2	1.9
CaO	0.39	0.29	0.37	0.11	0.2	0.27	0.2	0.22
Li_2O	0.06	0.26	0.08	0.09	0.1	0.21	0.29	0.55
Na_2O	0.33	0.11	0.13	0.1	0.05	0.11	0.07	0.07
K_2O	8.5	8.4	8.3	8.4	8.1	8.2	8.3	8.2
Rb_2O	0.062	0.112	0.071	0.074	0.076	0.078	0.095	0.176
Cs_2O	0.049	0.033	0.035	0.023	0.023	0.023	0.031	0.055
F	0.60	0.93	0.6	0.37	0.32	0.57	0.75	0.35
Cl	n.a.	n.a.	0.08	n.a.	n.a.	0.22	0.10	n.a.
Cations normalized to 22 oxygens								
Si	5.541	5.537	5.307	5.431	5.249	5.542	5.468	5.256
IV	2.459	2.463	2.693	2.569	2.751	2.458	2.532	2.744
Ti	0.326	0.331	0.456	0.408	0.462	0.391	0.356	0.282
Al^{VI}	0.147	0.29	0.021	0.504	0.37	0.186	0.142	1.091
Fe^{3+}	0.166	0.228	0.345	0.213	0.331	0.309	0.452	0.212
Fe^{2+}	1.035	1.966	2.5	2.584	2.804	3.601	3.783	3.256
Mn	0.014	0.107	0.061	0.039	0.075	0.074	0.09	0.106
Mg	4.117	2.758	2.388	1.873	1.621	1.041	0.778	0.443
Li	0.036	0.159	0.05	0.056	0.063	0.137	0.19	0.346
Sum [Y]	5.841	5.838	5.822	5.677	5.725	5.74	5.792	5.736
Ca	0.062	0.047	0.062	0.018	0.034	0.047	0.035	0.037
Na	0.096	0.032	0.039	0.03	0.034	0.035	0.022	0.021
K	1.619	1.625	1.648	1.663	1.629	1.7	1.728	1.636
Rb	0.006	0.011	0.007	0.007	0.008	0.008	0.01	0.018
Cs	0.003	0.002	0.002	0.002	0.002	0.002	0.002	0.004
Sum [X]	1.786	1.718	1.758	1.72	1.705	1.791	1.797	1.716
F	0.283	0.446	0.295	0.182	0.159	0.293	0.387	0.173
Cl			0.020			0.060	0.027	
mgli	4.08	2.6	2.34	1.82	1.56	0.9	0.59	0.1
feal	1.39	2.34	3.34	2.74	3.3	4.19	4.54	2.77
Variety	phlogopite	Mg biotite	Mg biotite	Fe biotite	Fe biotite	lepidomelane	lepidomelane	siderophyllite

(*Contd on next page*)

Region	Erzgebirge	Erzgebirge	Erzgebirge	Erzgebirge	Erzgebirge	Erzgebirge	Granulitgebirge
Locality	Schellerhau	Eibenstock	Pobershau	Altenberg	Eibenstock	Zinnwald	Penig
Rock type	monzogranite	Li mica syenogranite	Li mica syenogranite	greisen	Li mica syenogranite	greisen	pegmatite
Sample	8	24	20039	51	17	8184	1015
SiO_2	39.5	38.6	38.8	42.3	42.7	46.3	50.3
TiO_2	2.1	1.8	0.8	0.78	0.6	0.17	0.13
Al_2O_3	21.0	21.8	23.0	20.5	22.4	19.4	22.7
Fe_2O_3	1.51	1.05	1.05	1.58	0.2	0.79	0.79
FeO	18.40	18.10	15.93	13.90	13.80	9.64	1.28
MnO	0.45	0.33	0.20	0.68	0.35	1.13	1.51
MgO	1.03	1.3	0.8	1.3	0.58	0.1	0.03
CaO	0.17	0.14	0.19	0.2	0.14	0.24	0.16
Li_2O	0.88	1.3	1.8	2.3	2.9	3.9	5.6
Na_2O	0.17	0.15	0.17	0.22	0.2	0.25	0.25
K_2O	9.1	9.8	10.0	9.1	10.3	9.3	10.2
Rb_2O	0.329	0.509	0.598	0.827	0.767	0.867	1.424
Cs_2O	0.058	0.129	0.177	0.062	0.194	0.026	0.149
F	2.8	1.4	3.1	6.0	5.5	6.5	4.5
Cl	n.a.	0.06	n.a.	n.a.	n.a.	n.a.	n.a.
Cations							
Si	5.939	5.803	5.849	6.243	6.186	6.712	6.794
Al^{IV}	2.061	2.197	2.151	1.757	1.814	1.288	1.206
Ti	0.237	0.203	0.091	0.087	0.065	0.019	0.013
Al^{VI}	1.661	1.666	1.936	1.809	2.011	2.026	2.408
Fe^{3+}	0.17	0.119	0.119	0.175	0.022	0.086	0.08
Fe^{2+}	2.313	2.275	2.008	1.715	1.671	1.168	0.144
Mn	0.057	0.042	0.026	0.085	0.043	0.139	0.173
Mg	0.231	0.291	0.18	0.286	0.125	0.022	0.007
Li	0.532	0.786	1.091	1.365	1.689	2.273	3.042
Sum [Y]	5.201	5.383	5.451	5.522	5.627	5.733	5.866
Ca	0.027	0.023	0.031	0.032	0.022	0.037	0.023
Na	0.05	0.044	0.05	0.063	0.056	0.07	0.065
K	1.745	1.879	1.923	1.713	1.903	1.72	1.757
Rb	0.032	0.049	0.058	0.078	0.071	0.081	0.124
Cs	0.004	0.008	0.011	0.004	0.012	0.002	0.009
Sum [X]	1.858	2.003	2.073	1.890	2.065	1.910	1.978
F	1.331	0.666	1.478	2.8	2.519	2.979	1.922
Cl		0.016					
mgli	−0.30	−0.49	−0.91	−1.08	−1.56	−2.25	−3.03
feal	1.12	0.97	0.31	0.25	−0.21	−0.62	−2.00
Variety	siderophyllite	protolithionite	protolithionite	protolithionite	zinnwaldite	zinnwaldite	lepidolite

n.a. - Not analysed, mgli = Mg−Li (octahedral), feal = Fe(tot) + Mn + Ti−Al^{VI} (octahedral)

Analytical conditions are given in Tischendorf *et al.* (1969). The values for Si, Al, Ca, Na, Rb and Cs were recently re-analyzed by XRF and INAA, and modified accordingly.

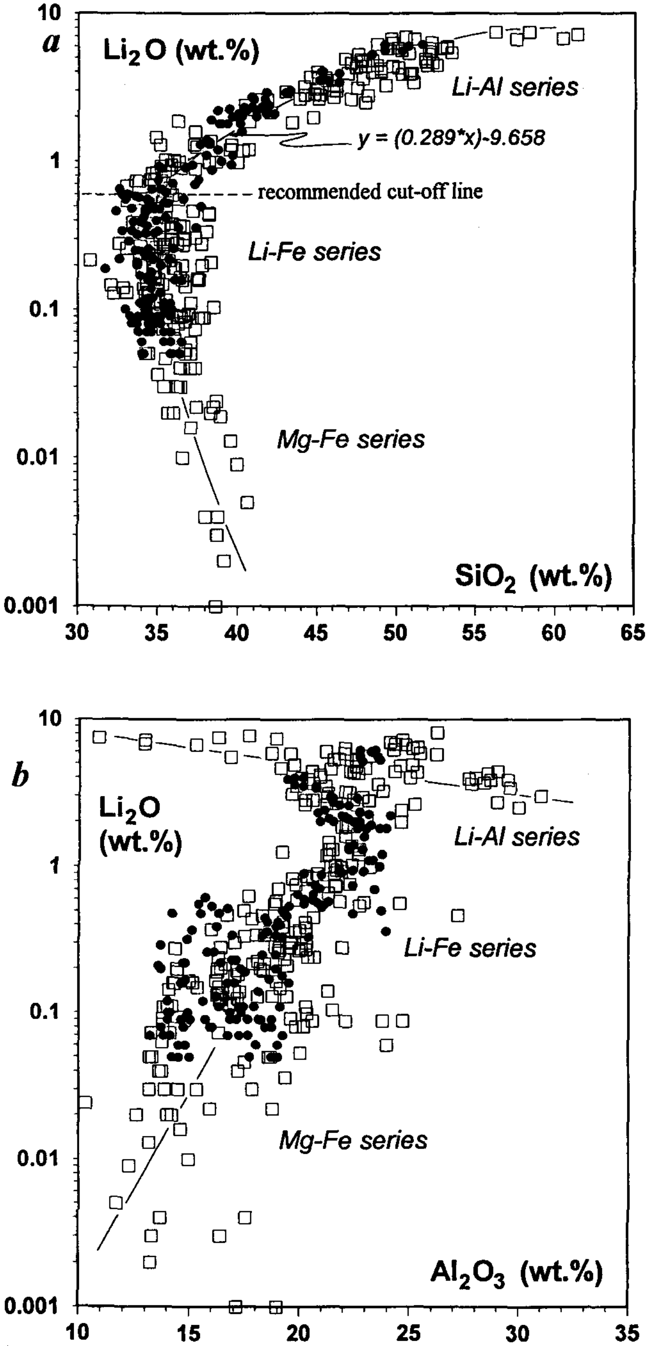

FIG. 4*a–f*. Variation of Li_2O with SiO_2 (*a*), Al_2O_3 (*b*), MnO (*c*), FeO_{tot} (*d*), TiO_2 (*e*), and MgO (*f*) in trioctahedral micas. Dots mark analyses from the authors (n = 169), open squares mark analyses from the literature (n = 256 – 267).

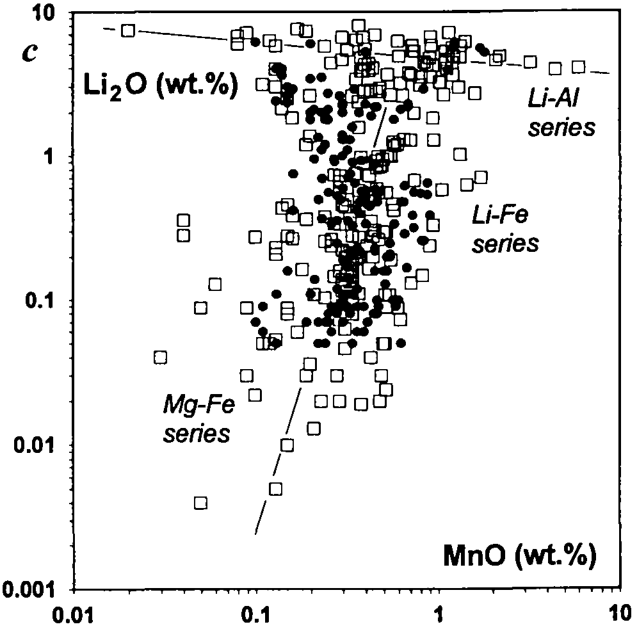
c
Li$_2$O (wt.%)
Li-Al series
Li-Fe series
Mg-Fe series
MnO (wt.%)
10
1
0.1
0.01
0.001
0.01
0.1
1
10

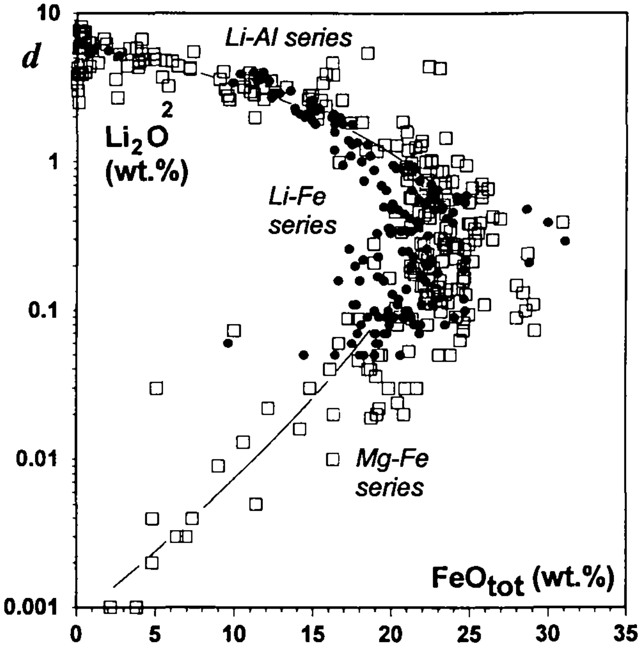
d
Li-Al series
Li$_2$O (wt.%)
2
Li-Fe series
Mg-Fe series
FeO$_{tot}$ (wt.%)
10
1
0.1
0.01
0.001
0
5
10
15
20
25
30
35

Fig. 4. Contd.

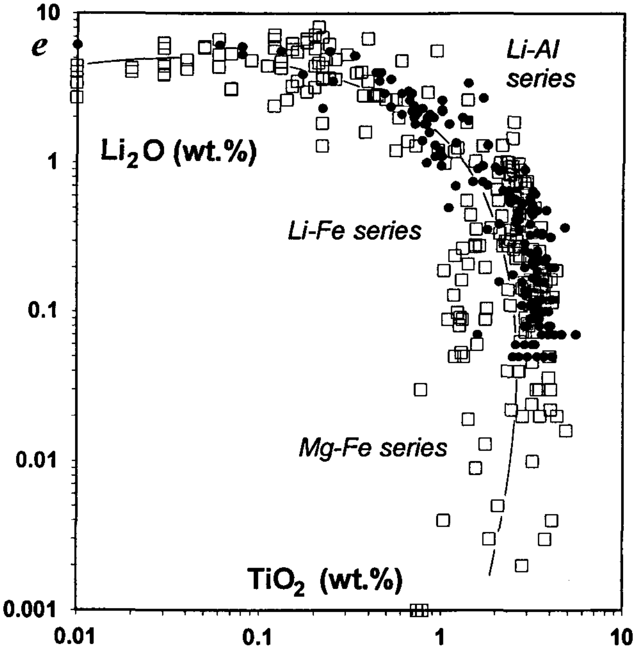
e
Li$_2$O (wt.%)
TiO$_2$ (wt.%)
Li-Al series
Li-Fe series
Mg-Fe series
10
1
0.1
0.01
0.001
0.01
0.1
1
10

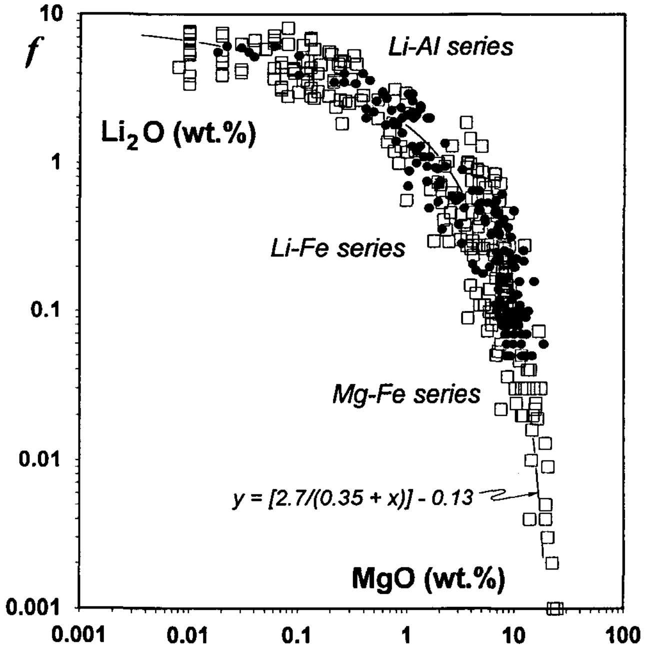
f
Li$_2$O (wt.%)
MgO (wt.%)
Li-Al series
Li-Fe series
Mg-Fe series
y = [2.7/(0.35 + x)] - 0.13
10
1
0.1
0.01
0.001
0.001
0.01
0.1
1
10
100

Fig. 4. Contd.

TABLE 2. Compilation of regression equations for estimating Li_2O contents in tri- and dioctahedral micas

Equation	Li_2O (wt.%)	Number of analyses (n)	Goodness of fit parameter (R^2)	Range of validity (wt.%)
[tri 1]*	$= (0.289*SiO_2) - 9.658$	232	0.912	$SiO_2 > 34$; $MgO < 6$
[tri 2]*	$= [2.7/(0.35 + MgO)] - 0.13$	434	0.880	$MgO = 0.01$ to 20
[tri 3]**	$= 155*MgO^{-3.1}$	191	0.58	$SiO_2 > 34$; $MgO > 6$
[tri 4]	$= 0.237*F^{1.544}$	501	0.852	$F = 0.1$ to 9
[tri 4a]	$= (0.697*F) + 1.026$	62	0.70	aplites, pegmatites
[tri 4b]	$= 0.177*F^{1.642}$	439	0.906	granitoids a.o.
[tri 5]	$= 3.5*Rb_2O^{1.55}$	470	0.865	$Rb_2O = 0.01$ to 1.7
[di 1]*	$= 0.3935*F^{1.326}$	199	0.843	$F = 0.01$ to 8
[di 2]	$= 1.579*Rb_2O^{1.45}$	209	0.71	$Rb_2O = 0.01$ to 2

* - recommended ** - recommended in combination with eq. [tri 1]

We note that some mica analyses from a few occurrences (not plotted in Fig. 4*f*) deviate from this relationship. In these, at a given MgO content, the concentration of Li_2O is displaced towards either higher (Černý *et al.*, 1970; Černý and Trueman, 1985; Neiva, 1981*a*; Henderson *et al.*, 1989) or lower values (Goeman, 1972; Rub *et al.*, 1986; Nash, 1993; du Bray, 1994; Černý *et al.*, 1995; Rieder *et al.*, 1996) than would be calculated by equation [tri 2]. The reason for the deviations is not clear. It may include analytical problems (for example, the data of Henderson *et al.*, 1989, are from SIMS analyses, which systematically overestimate Li, see Ottolini *et al.*, 1993); and/or particular conditions of formation (F-rich annitic biotites from the Honeycomb Hills rhyolite, Utah, apparently formed or reequilibrated at high F and O fugacity; see Nash, 1993 and Icenhower and London, 1997).

One of the problems encountered by Tindle and Webb (1990) was the poor correlation between Li and Si at higher MgO compositions. For micas with MgO greater than 6 wt.%, we obtained the following expression relating Li_2O and MgO:

$$Li_2O = 155MgO^{-3.1} \ (R^2 = 0.58;\ n = 191) \quad [\text{tri } 3]$$

The chemical correlation between Li and F in trioctahedral micas is good. This is well known, and Tindle and Webb (1990) presented an equation linking the two variables with R^2 of 0.617. Figure 5*a* shows the relations of Li and F in trioctahedral micas. Use of all analyses results in the following equation:

$$Li_2O = 0.237F^{1.544} \ (R^2 = 0.852,\ n = 501) \quad [\text{tri } 4]$$

Close examination of Fig. 5*a* shows that micas from pegmatites and aplites define an array which differs in slope from that of the micas contained in granitoids and other rocks. If we divide the data set into two groups we obtain, for pegmatites and aplites using data from Černý *et al.* (1970, 1995), Rieder (1970), Bargar *et al.* (1973), Chaudhry and Howie (1973), Skosyreva and Vlasova (1983), Edmunds *et al.* (1985), Jolliff *et al.* (1987), Henderson *et al.* (1989), Neiva and Gomes (1991) and from our data set:

$$Li_2O = (0.697F) + 1.026 \ (R^2 = 0.70,\ n = 62) \quad [\text{tri } 4a]$$

and for the micas in granitoids and other rocks:

$$Li_2O = 0.177F^{1.642} \ (R^2 = 0.906,\ n = 439) \quad [\text{tri } 4b]$$

Finally, Fig. 5*b* displays the positive correlation of lithium and rubidium in trioctahedral micas. The correlation is excellent except for micas with very low values of Li_2O and Rb_2O. The data can be fit by the following regression equation:

$$Li_2O = 3.5*Rb_2O^{1.55} \ (R^2 = 0.865,\ n = 470) \quad [\text{tri } 5]$$

Dioctahedral micas. Compared with the trioctahedral micas, there are much fewer published analyses of dioctahedral Li micas and also fewer elements in the micas for which a correlation with lithium can be tested. Our data compilation for the dioctahedral micas includes, in addition to unpublished data from our own and R. Naumann, published analyses for micas designated as muscovite, Li-muscovite, Li-phengite and Al–Li micas including mixed forms (see Appendix).

No systematic variation of Li_2O with either SiO_2 or Al_2O_3 (not shown) was found, and we present diagrams here only for Li–F and Li–Rb (Fig. 6*a*–*b*). Fluorine shows a good positive correlation with lithium over the full compositional range, as was the case for trioctahedral micas. The Li–F relationship can be defined by the following relation:

$$Li_2O = 0.3935F^{1.326} \ (R^2 = 0.843,\ n = 199) \quad [\text{di } 1]$$

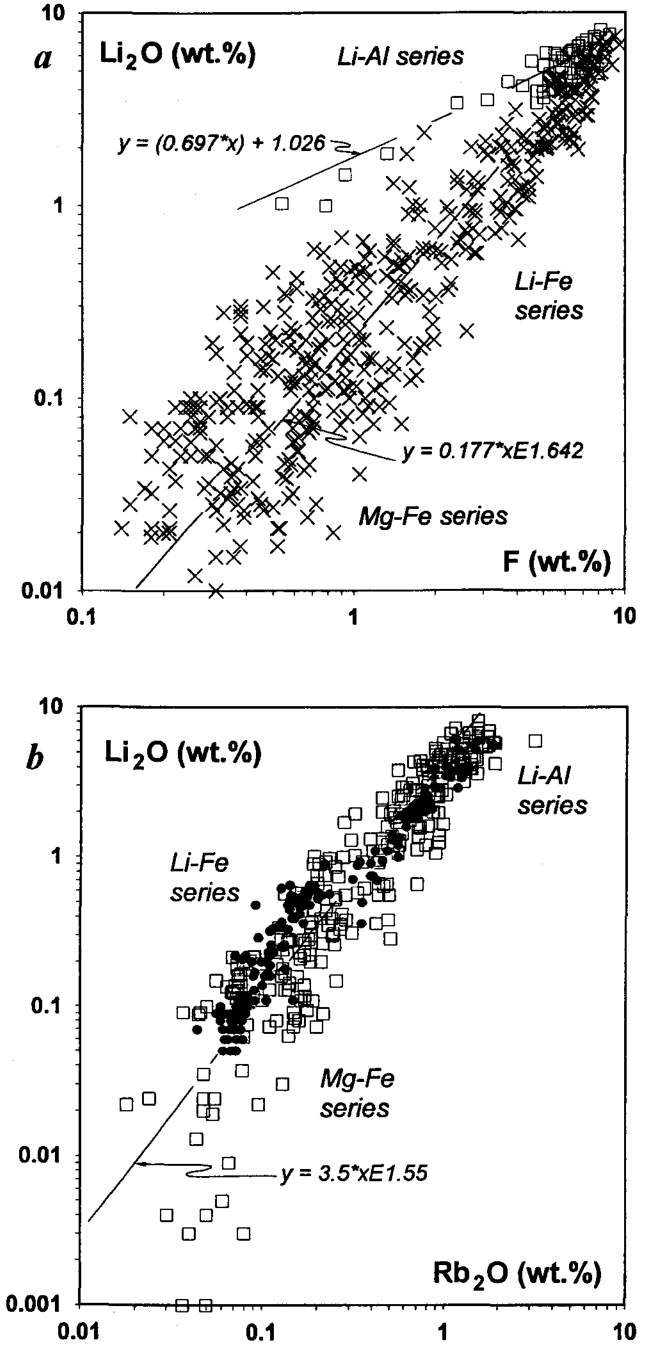

FIG. 5*a–b*. Variation of Li_2O with F (*a*) and Rb_2O (*b*) in trioctahedral micas. (*a*): Open squares denote aplites and pegmatites ($n = 62$). Crosses denote granitoids and other rocks ($n = 439$). (*b*): Dots mark analyses from the authors ($n = 178$), open squares mark analyses from the literature ($n = 292$).

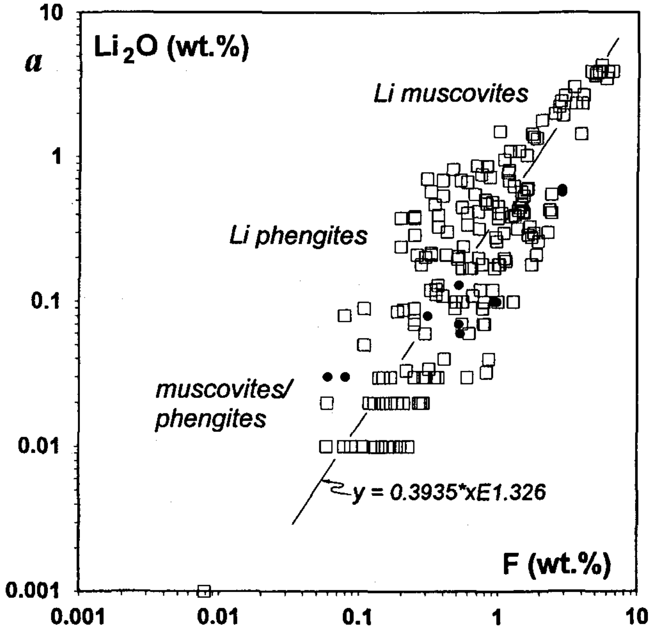

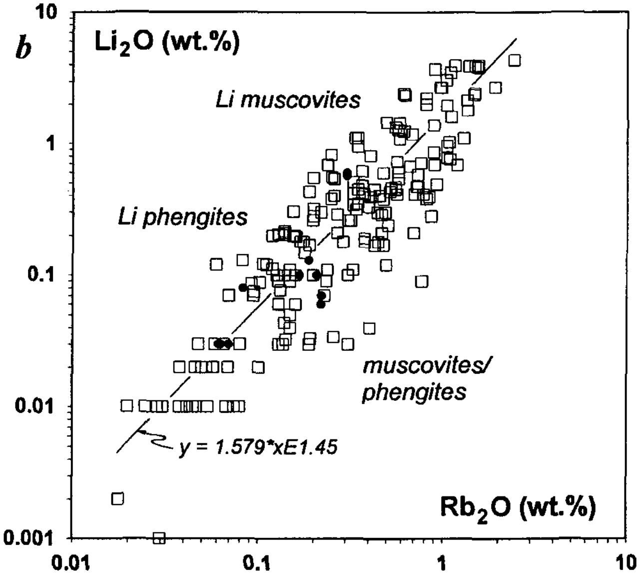

FIG. 6a–b. Variation of Li_2O with F (a) and Rb_2O (b) in dioctahedral micas. Dots mark analyses from the authors (n = 12), open squares mark analyses from the literature (n = 187 and 197, resp.).

The Li–Rb correlation is slightly worse, and can be expressed as follows :

$Li_2O = 1.579Rb_2O^{1.45}$ ($R^2 = 0.71$, $n = 209$) [di 2]

Summary. Tindle and Webb (1990) concluded that Li can best be estimated from microprobe analyses of lithium-bearing trioctahedral micas using the correlation with SiO_2. Our compilation of Li-mica analyses confirms this relationship and provides additional information. Table 2 compiles all the equations we have discussed above which relate Li to other components which (with the exception of Rb), are routinely and reliably analysed by electron microprobe. Although we have used a data set different from that of Tindle and Webb (1990), the equations for the Li_2O-SiO_2 relation are essentially identical and point to their universal applicability. In addition to this, we offer other correlation equations, particularly for high-Mg micas with compositions outside the range dealt with by Tindle and Webb.

In our experience, equation [tri 1] gives the best results for micas with greater than 36 wt.% SiO_2 and less than 6 wt.% MgO. For micas outside this range one can use either [tri 3] (for MgO-rich micas) or [tri 2], which is applicable over the whole range of MgO. Equation [tri 2] is recommended for micas with less than 36 wt.% SiO_2.

We present the first equation which quantifies the relationships between Li and F for trioctahedral micas alone, and is based on a comparatively large number of analyses. The Li–F regression calculated by Tindle and Webb (1990) incorporated data from both trioctahedral and dioctahedral micas, which is the main reason for the relatively poor 'goodness of fit' recognized. A good approximation for Li in trioctahedral micas can also be obtained if data for Rb are available.

Furthermore, we present equations applicable to dioctahedral micas, for predicting Li contents based on the F or Rb concentration, a group for which Tindle and Webb (1990) found insufficient data to make a reliable assessment of element correlations. Both equations can be used, however, the Li–Rb correlation is less good than Li–F.

Mica classification and graphical representation

Principles. Graphical representations of mineral compositions should be simple and practical to use, even for the non-specialist. They should allow classification of the mineral species and also show the important compositional changes of the minerals in response to evolution of the host rocks (e.g. prograde metamorphism, igneous fractionation). There are a number of graphical schemes in use for the micas, but we find that none of these is ideally suited for the study of Li micas, for the reasons given below.

The classical triangular diagrams of Foster (1960*a,b*) meet the above criteria for most purposes, and they are widely used. However, for the Li-micas, Foster's representation has the disadvantage that it separates the Mg–Fe micas (phlogopite, biotite, siderophyllite and lepidomelane) from the lithian varieties (protolithionite, zinnwaldite, lepidolite and Li-muscovite), and requires the use of two classification triangles with: Mg^{2+}; $Fe^{2+} + Mn^{2+}$; $Al^{VI} + Fe^{3+}$ + Ti; and Li; $Mg^{2+} + Fe^{2+} + Mn^{2+}$; $Al^{VI} + Fe^{3+}$ + Ti (see Fig. 2), respectively. Tröger (1962) also treated the Li micas and the Mg–Fe micas as two separate series. This is a problem when one studies micas in composite granite plutons, whose whole-rock compositions vary from fairly primitive to highly evolved. Both Li micas and Mg–Fe micas coexist in many of these granites and there is appreciable Li even in the latter, so that the treatment of these mica groups in separate diagrams makes it difficult to see the relationships between them. Rieder (1970) was the first to combine the Li micas with the Fe–Mg micas in one classification diagram, a tetrahedron with the corner points Mg (phlogopite), $Fe^{2+} + Mn^{2+}$ (annite), $Al^{VI} + Fe^{3+} + Cr^{3+}$ (muscovite) and Li/$R^{3+;VI}$ (trilithionite). In practice, this requires using four 2-dimensional projections. Also, taenolite and polylithionite lie outside the range of the diagram and Ti is not accounted for. Monier and Robert (1986*b*) also introduced a mica tetrahedron with the components M^{2+}, Li, Al and Si. Their scheme has the important disadvantage of combining Mg and Fe^{2+} into one variable. Gottesmann and Tischendorf (1978) proposed a classification diagram based on a double triangle with the following corner variables: Mg–Li (phlogopite), Li–Mg (near-lepidolite), $Al^{VI} + Fe^{3+}$ + Ti (muscovite) and $Fe^{2+} + Mn^{2+}$ (annite). Drawbacks of this classification scheme are that Ti and Fe^{3+} are assigned to the muscovite component, as in Foster (1960*a,b*), which is not geochemically justified, and that ferric and ferrous iron are plotted separately. Černý and Burt (1984) proposed a vector representation of mica composition which also incorporated vacancies in the octahedral layer. Their emphasis was on micas in granitic pegmatites, and they considered only the components K-Li-Fe-Al-Si. This limits application of this scheme to mica varieties with negligible amounts of Mg, Mn and Ti.

We propose a new diagram which has particular advantages for representing the composition of Li micas. The diagram is based on the octahedral cations in micas, and these are cast into four components according to geochemical reasoning and the element correlations in natural micas which were discussed above: Mg, Li, Al^{VI}, and Fe_{tot} + Ti + Mn. We draw attention to the fact that *titanium* is treated here as a member of the iron-group and not, as usual, added to Al^{VI}. The reason for this is that

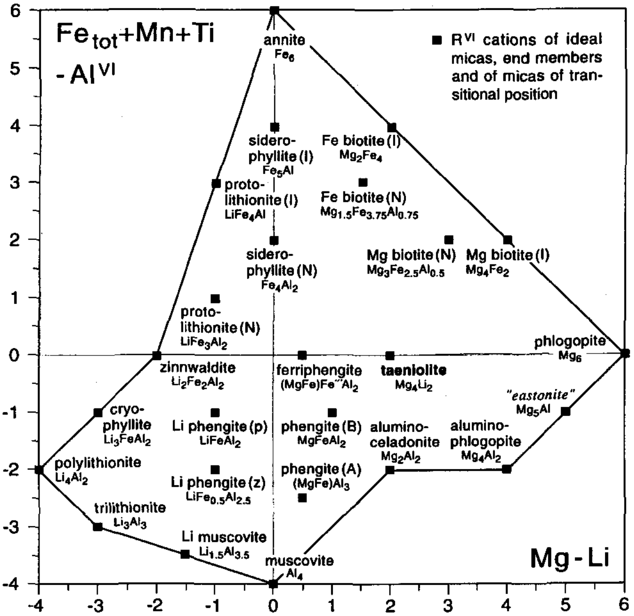

FIG. 7. Position of ideal mica end-members and selected intermediate compositions in the diagram [Mg–Li] *vs.* [Fe_{tot} + Mn + Ti–Al^{VI}]. See text for further details.

titanium correlates positively with total iron (R = 0.676, n = 201, own data set), but negatively with the six-fold coordinated alumina (R = –0.895; n = 201). The variables on both the x- and y-axes are combinations of two components each, making it possible to display the effects of four components (albeit not separately) on a two-dimensional diagram. The axis variables are [Mg minus Li] and [Fe_{tot} plus Mn plus Ti minus Al^{VI}]. These take account of the need to show Mg and Fe variations separately and are based on the strong, constant negative correlations in mica which we observe between Mg and Li on the one hand, and Fe_{tot} and Al^{VI} on the other. The parameter [Mg–Li] reflects the proportions of the phlogopite and polylithionite components, and the parameter [Fe_{tot} + Mn + Ti–Al^{VI}] reflects the proportions of the annite and muscovite components.

This diagram has a number of useful features. First, the full range of micas from Li-bearing to Li-free can be plotted on the same diagram. Second, in contrast to triangular plots, it shows true and not relative concentrations. Third, because it takes into account all of the important octahedral cations, the total occupancy of the octahedral sites can be read off the diagram and relations between the trioctahedral and dioctahedral micas are easy to see.

Figure 7 shows the position of ideal mica compositions in the diagram. For Fe and Mg biotites, siderophyllite and protolithionite, two compositions are shown; one (I) is the ideal formula; the other (N) represents an average natural composition (vacancy-free). For phengites, two formulae are given (A, B). We have also added three intermediate compositions, Li phengite(p) at $LiFeAl_2$, Li phengite(z) at $LiFe_{0.5}Al_{2.5}$, and Li muscovite at $Li_{1.5}Al_{3.5}$ to emphasize the natural transitions between muscovite and protolithionite, zinnwaldite and tri- to polylithionite, respectively. The composition of taeniolite (Mg_4Li_2) is anomalous. It is a trioctahedral mica which, because of the lack of Fe, Mn, Ti and Al, plots at zero on the Y-axis. The same point would be occupied by a mica with $Mg_2Fe_{1.25}Al_{1.25}$ and R^{VI} = 4.5 (see Fig. 8 below), which has not been previously described. Taeniolite apparently requires exceptional conditions of formation where lithium-rich alkaline fluids interact with high-Mg rocks (such as fenites and carbonatites, see Ganzeeva, 1973 and Cooper *et al.*, 1995). Note that the hypothetical end-member eastonite is put in quotation marks in the figure because natural 'eastonite' actually consists of a mixture of phlogopite and serpentine (Livi and Veblen, 1987).

It has long been known that the trioctahedral micas can cover the whole range in composition from the Mg-rich to the Li-rich varieties, but there are also transitions with the dioctahedral micas (Monier and Robert, 1986*b*), which are favoured by the presence

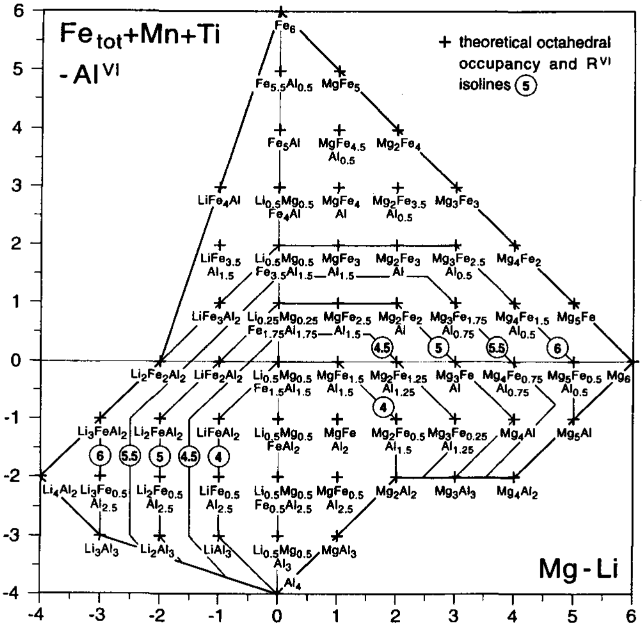

FIG. 8. Theoretical octahedral occupancy in micas (Fe in octahedral occupancy = Fe_{tot} + Mn + Ti) and lines of constant octahedral sum (R^{VI}) based on the unit cell $X_2Y_{4-6}Z_8O_{20}(OH,F)_4$ in the [Mg–Li] *vs*. [Fe_{tot} + Mn + Ti–Al^{VI}] diagram.

of high Li (and/or perhaps F). To aid in recognizing transitions between tri- and dioctahedral micas, Figure 8 shows all theoretical cation occupancies of the octahedral layer in the diagram, and we have added lines of constant octahedral sum (R^{VI}). It is customary to consider micas with R^{VI} from 5.0 to 6.0 as trioctahedral, and micas with R^{VI} near 4.0 as dioctahedral. We find it appropriate to fix a value for R^{VI} = 4.4 as the division between dioctahedral and trioctahedral micas (see also Monier and Robert, 1986*a*).

Figure 9 shows the compositional range of naturally-occurring, common mica species on the proposed diagram. The compositional ranges for the trioctahedral mica species follow the suggestions of Foster (1960*a*,*b*). We have simply transposed the Mg and Li values to fit our axis variables, so the existing nomenclature remains unchanged. The lines at x = 0 and y = 0 divide the diagram into four quadrants, which correspond to the Mg–Fe micas (quadrant I), Mg–Al micas (quadrant II), Li–Al micas (quadrant III) and Li–Fe micas (quadrant IV). Also shown is the line of R^{VI} = 4.4, which divides the fields of the dioctahedral and trioctaheral micas. Details about the range of specific mica species are discussed briefly below, and the reader is referred to Table 3 for a compilation of the boundary values.

Most phlogopites ([Mg–Li] > 4) are relatively aluminum-poor and plot in quadrant I, although there are also some Al-enriched phlogopites, which plot in the field labelled alumino-phlogopite. The fields of Mg and Fe biotites are divided by the value [Mg–Li] = 2 and, additionally, by a dotted line which corresponds to Foster's (1960*a*) criterion of whether Fe or Mg is the dominant octahedral cation. The lower end of the biotite field is defined by the trioctahedral/dioctahedral boundary at R^{VI} = 4.4. Lepidomelane was defined by Foster (1960*a*) at Fe^{3+} > Al^{VI} and Mg < 0.3. The lepidomelane field in our diagram is bounded by the condition [Fe_{tot} + Mn+ Ti–Al^{VI}] > 4. The siderophyllite field crosses quadrants I and IV, with a range of [Mg–Li] values from –0.4 to 0.6. Like biotite, the lower end of the siderophyllite field is defined by the trioctahedral/dioctahedral boundary. Protolithionite (Winchell, 1942; Foster, 1960*b*) is a mica species with relatively high lithium contents and Fe_{tot} + Mn + Ti > Al^{VI}. Rieder (1970) suggested that the term be disused as a mica variety because there are no natural micas with the ideal composition of $LiFe_4Al$. We

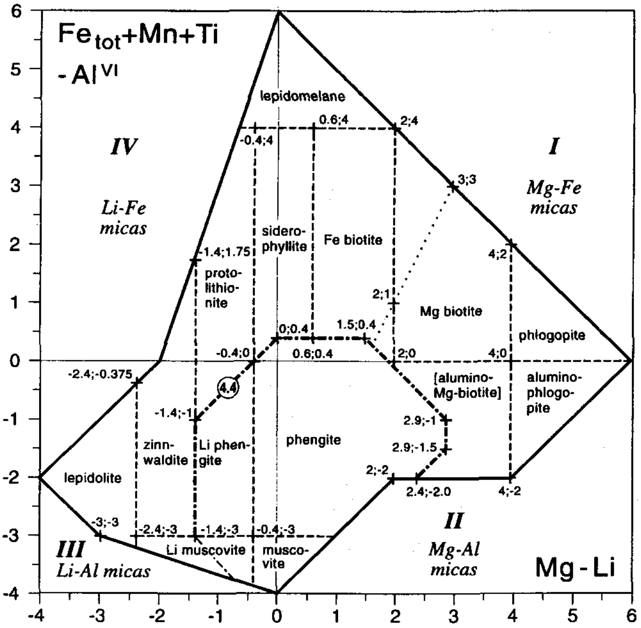

FIG. 9. Compositional fields of natural trioctahedral and dioctahedral micas on the diagram of [Mg−Li] *vs.* [Fe$_{tot}$ + Mn + Ti−Al^{VI}], with R^{VI} = 4.4 as the boundary between di- and trioctahedral micas. The dotted line shows the discrimination boundary between Mg and Fe biotite from Foster (1960a). Quadrants I, II, III and IV correspond to the mica series Mg−Fe, Mg−Al, Li−Al and Li−Fe, respectively.

believe it is useful to retain a protolithionite field (see also Gottesmann and Tischendorf, 1980) and suggest that protolithionite is better represented by the composition $LiFe_3Al_2$ (see Fig. 7). Zinnwaldites are not only Li-richer than protolithionites, but they are also generally Al-richer and plot in quadrant III. There are, however, some zinnwaldites with [Fe$_{tot}$ + Mn + Ti−Al^{VI}] = 0 to 0.5, and some protolithionites where this value is as low as −0.5. Lepidolites, which can be considered as a collective name for the most Li-rich micas including polylithionite, trilithionite (= paucilithionite), and cryophyllite plot exclusively in quadrant III and are bounded from zinnwaldite by the condition [Mg−Li] < −2.4.

TABLE 3. Compositional range of mica varieties with respect to [Mg−Li] and [Fe$_{tot}$ + Mn + Ti−Al^{VI}], and other important element relations

Variety	Mg−Li	Fe$_{tot}$ + Mn + Ti−Al^{VI}	Element relations
Phlogopite	6.0 ... 4.0	2.0 ... 0	Mg ≫ Fe$_{tot}$
Mg biotite	4.0 ... 2.0	2.0/4.0 ... 0	Mg > Fe$_{tot}$
Fe biotite	2.0 ... 0.6	4.0 ... 0.4	Fe$_{tot}$ > Mg
Lepidomelane	2.0 ... −0.6	6.0 ... 4.0	
Siderophyllite	0.6 ... −0.4	4.0 ... 0.4(0)	
Protolithionite	−0.4 ... −1.4	4.0(1.75) ... −1.0(0)	Fe$_{tot}$ > Li
Zinnwaldite	−1.4 ... −2.4	1.75(−0.375) ... −3.0	Li ~ Fe$_{tot}$
Lepidolite	−2.4 ... −4.0	−0.375 ... −3.0	Li > Fe$_{tot}$
Li phengite	−0.4 ... −1.4	(0)−1.0 ... −3.0	Li ~ Fe$_{tot}$
Li muscovite	−0.4 ... −2.4	−3.0 ... −3.8	Li ≫ Fe$_{tot}$
Muscovite	1.0 ... −0.4	−3.0 ... −4.0	Al^{VI} ≫ Fe$_{tot}$

We find it appropriate to define a field for Li phengites in quadrant III, to include dioctahedral micas with values of [Mg–Li] between −1.4 and −0.4 (analogous to the protolithionite boundaries). Micas of this composition are fairly common (see Lapides *et al.*, 1977; Uhlig, 1992). Note that the line at [Mg–Li] = −1.4, which divides the Li phengite field from zinnwaldite, coincides exactly with the value of R^{VI} = 4.4 for the dioctahedral/trioctahedral boundary. This confirms the usefulness of both boundary values. The Li phengites are succeeded, at a value of [Fe_{tot} + Mn + Ti–Al^{VI}] < −3, by the field of Li muscovite. Micas of the structurally 'mixed forms', which Foster (1960*b*, Fig. 39) attributed to immiscibility between dioctahedral and trioctahedral mica, plot in this field. The 'mixed forms' cover the same range of Li concentrations as zinnwaldite, and therefore we extend the field of Li muscovite out to a value of [Li–Mg] = −2.4. The muscovite field is defined at [Mg–Li] > −0.4 and [Fe_{tot} + Mn + Ti–Al^{VI}] < −3. It is bounded upward in the diagram by the large phengite field, which covers nearly the entire dioctahedral portion of the Mg–Al mica field (quadrant II) and extends slightly into quadrants III and I. Due to a lack of sufficient Li analyses, quadrant II will not be treated here in more detail. Theoretically, trioctahedral micas compositionally resembling alumino-Mg biotite should form in nature. However, according to the authors' knowledge, natural occurrences are not yet known.

Lapides *et al.* (1977) and Sun Shihua (1984) have already emphasized that transitions between dioctahedral and trioctahedral micas exist. We can best show the extent of this by plotting the sum of octahedral cations (R^{VI}) against the axis variables [Mg–Li] and [Fe_{tot} + Mn + Ti–Al^{VI}] (Figs. 10 and 11). Figure 10 shows that most of the trioctahedral micas have R^{VI} values between 5 and 6, with the lowest values and the greatest spread at intermediate values of [Mg–Li] between −2 and 2. Very prominent in the figure is a continuous series between lepidolite/zinnwaldite ([Mg–Li] = −3 to −2, R^{VI} = 6 to 5) and muscovite ([Mg–Li] = 0, R^{VI} = 4), which is explained by the experimental demonstration of solid solution between muscovite and zinnwaldite by Monier and Robert (1986*b*). Figure 11 shows the extent of transitions in natural mica compositions between dioctahedral muscovite/phengite (R^{VI} = 4, [Fe_{tot}+ Mn + Ti–Al^{VI}] = −3 to

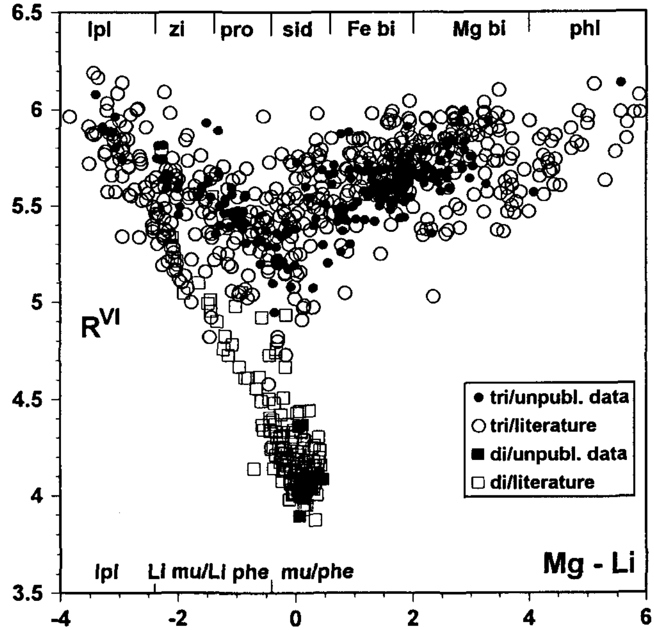

FIG. 10. Compositions of natural micas in terms of [Mg–Li] and octahedral occupancy (R^{VI}). The continuous transition of dioctahedral micas between muscovite ([Mg–Li] = 0) and zinnwaldite/lepidolite ([Mg–Li] = −2 to −4) is discussed in the text. The number of trioctahedral micas plotted is 730, dioctahedral micas: 212. Abbreviations here and in Figs. 11 and 12: Al phl = aluminophlogopite, Fe bi = Fe biotite, Li mu = Li muscovite, Li phe = Li phengite, lpm = lepidomelane, lpl = lepidolite, Mg bi = Mg biotite, mu = muscovite, phe = phengite, phl = phlogopite, pro = protolithionite, sid = siderophyllite, tae = taenolite, zi = zinnwaldite.

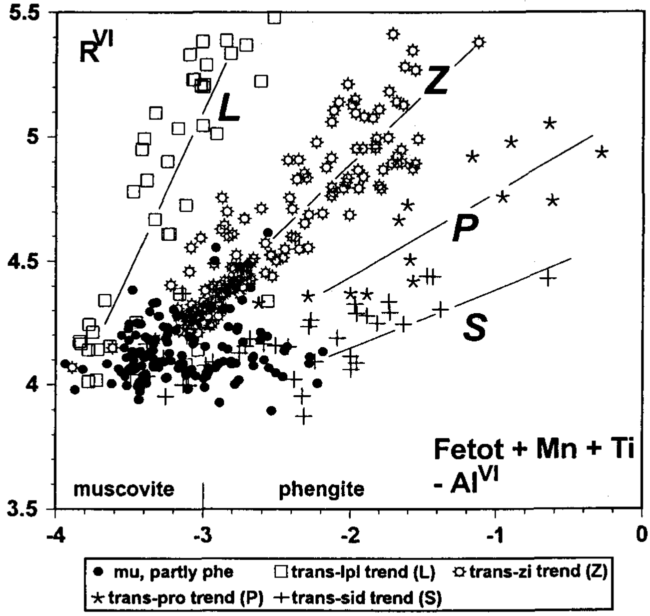

FIG. 11. Compositions of natural micas in terms of [Fe_{tot} + Mn + Ti–Al^{VI}] and octahedral occupancy (R^{VI}). We emphasize the extent of intermediate compositions between dioctahedral muscovite/phengite at R^{VI} = 4 and trioctahedral micas lepidolite (trend L), zinnwaldite (trend Z), protolithionite (trend P) and siderophyllite (trend S).

–4) and the trioctahedral micas lepidolite (trend L; data from Foster 1960*b*; Lapides *et al.*, 1977; Luecke 1981; Jolliff *et al.*, 1987), zinnwaldite (trend Z; data from Lapides *et al.*, 1977; and our data, see Fig. 13), protolithionite (trend P; data from Lapides *et al.*, 1977; Uhlig, 1992; du Bray, 1994; and our data) and siderophyllite (trend S; data from Lapides *et al.* 1977). We designate micas plotting along trend Z as Li-phengites (z), and those along trend P as Li phengites(p). Additional sources of data for Fig. 11 are given in the Appendix (column of Fig. 6).

Discussion and applications

Use of the proposed diagram (Fig. 9) requires, of course, that Li concentrations are either determined directly or can be estimated by correlation with other constituents of a microprobe analysis (using the correlations outlined in this paper and by Tindle and Webb, 1990). Note that very Mg-rich or Li-rich micas will be correctly classified by the diagram even without Li or Mg data, respectively, because the dominant cations define the position of the mica varieties.

The diagram can be used for the full range of mica compositions, except for those in which other octahedral cations such as Zn (hendricksite) and Mn (masutomilite) play a dominant or essential role. Figure 12 shows the position of a wide variety of natural micas. The groups of mica analyses are coded by a number to the following data sources:

[1] Phlogopites and Mg biotites from mafic igneous rocks (mantle xenoliths, kimberlites, gabbroic rocks, lamprophyres, nephelinites, melilites), and from metamorphic rocks (Métais *et al.*, 1962; Boettcher and O'Neil, 1980; De Fino *et al.*, 1983; Basu *et al.*, 1984; De Kimpe *et al.*, 1987; Wagner *et al.*, 1987; Malyshonok, 1989; Grew *et al.*, 1990; Edgar, 1992; Kramer and Seifert, 1994; Harlow, 1995).

[2] Mg biotites from granodioritic rocks (Neiva, 1981*a*; Bigi and Brigatti, 1994).

[3] Fe biotites from granitic rocks and contact metamorphic rocks (Müller, 1966; Barrière and Cotton, 1979; Bea, 1980; Neiva, 1980, 1981*b*). Some of the analyses from Barrière and Cotton (1979) plot in the lepidomelane field.

[4] Lepidomelanes from nepheline syenite pegmatites (Foster, 1960*a*), theralites (Mokhtari *et al.*, 1985: 'annite–ferriannite') and from granitic rocks of the Brocken pluton (Harz) and the Königshain massif (Lausitz) (see analysis 906 and 520 in Table 1) from the authors' unpublished data.

[5] Siderophyllite–protolithionite–zinnwaldite–lepidolite micas from evolved granitic bodies and tin deposits (Rieder, 1970; Rub *et al.*, 1983; Sun Shihua,

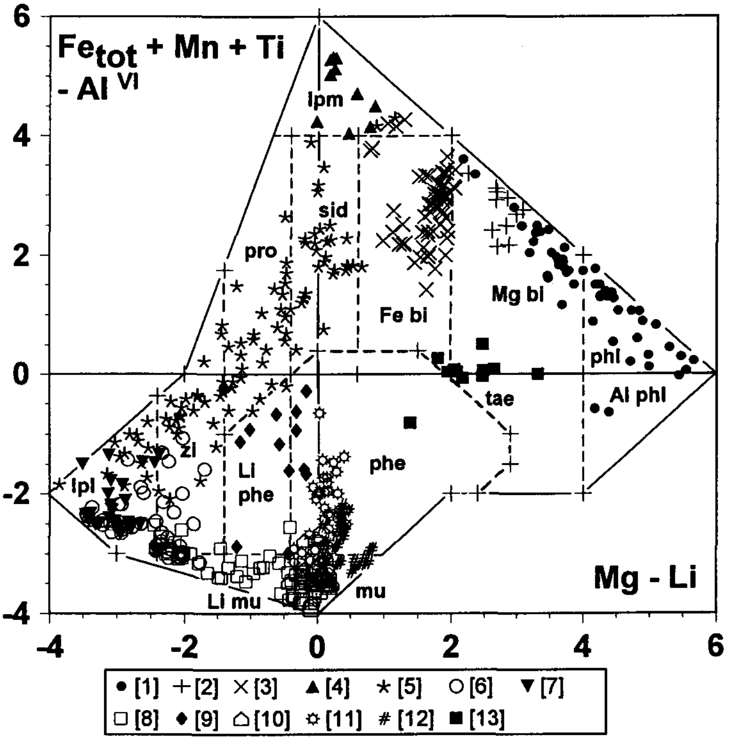

FIG. 12. Positions of the full range of natural micas on the diagram of [Mg–Li] *vs.*[Fe_{tot} + Mn + Ti–Al^{VI}]. The numbers in the legend refer to data sources and are explained in the text.

1984; Henderson *et al.*, 1989; Stone *et al.*, 1988; du Bray, 1994).

[6] Zinnwaldite and lepidolite from evolved granites and associated aplites and pegmatites (Chaudhry and Howie, 1973; Fonteilles, 1987; Jolliff *et al.*, 1987; Charoy *et al.*, 1995; Charoy and Noronha, 1996). Note that the micas designated as trilithionite (= lepidolite) by Charoy *et al.* (1995) have [Mg–Li] = –2.06 to –2.35 and therefore plot here as zinnwaldites.

[7] Lepidolites from a rare-metal albite leucogranite (Beauvoir granite), rare metal-enriched alkaline complexes, and pegmatites (Černý *et al.*, 1970, 1995; Černý and Trueman, 1985; Monier *et al.*, 1987; authors' unpublished data and analysis 1015 in Table 1).

[8] Li muscovites from two-mica granites, and pegmatites (Foster, 1960*b*; Lapides *et al.*, 1977; Luecke, 1981; Charoy *et al.*, 1995; Charoy and Noronha, 1996). Charoy *et al.* (1995) classified some of these as phengites (cores in zoned grains) but we would term them Li muscovites because they have [Fe_{tot} + Mn + Ti–Al^{VI}] below –3.2.

[9] Li phengites from highly fractionated granites (Lapides *et al.*, 1977) and from rocks of the tin deposit Ehrenfriedersdorf, Erzgebirge (Uhlig, 1992).

[10] Muscovites from two-mica granites and pegmatites (Müller, 1966; Lapides *et al.*, 1977; Henderson *et al.*, 1989; Silva and Neiva, 1990; Neiva and Gomes, 1991; Neiva, 1992; Černý *et al.*, 1995; Grew *et al.*, 1995; Rieder *et al.*, 1995).

[11] Phengites from highly fractionated granites (Lapides *et al.*, 1977 'phengite-muscovites').

[12] Phengitic muscovites from two-mica paragneisses (Naumann's and authors' unpublished data) and phengites from jadeite and mica-albite rocks (Harlow, 1995).

[13] Taeniolite from alkali-metasomatic zones (fenites) (Ganzeeva, 1973; Cooper *et al.*, 1995).

The goals of a particular study may make it useful to use only a portion of the proposed diagram or change the axis scaling. As an example, Fig. 13 shows the Li-rich portion of the diagram to illustrate the variation of trioctahedral and dioctahedral micas in the multi-phase Variscan Eibenstock granite, western Erzgebirge, Germany (cf. Fig. 1). The

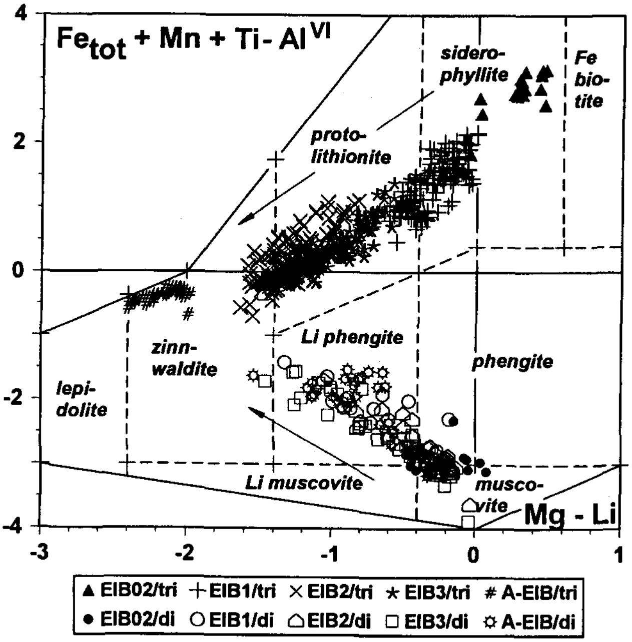

FIG. 13. Composition of micas from the Variscan Eibenstock granite, western Erzgebirge, shown in a portion of the diagram [Mg–Li] *vs.*[Fe_{tot} + Mn + Ti–Al^{VI}]. The samples are coded according to the granite subintrusions in which they occur (EIB0 to EIB3 are least evolved to most evolved facies and A-EIB is aplite), and according to trioctahedral (tri) or dioctahedral (di) composition. The arrows indicate evolution of mica compositions due to magma fractionation. Analyses by electron microprobe, Li-contents estimated using equations [tri 1] and [di 1] in Table 2.

micas were analysed by electron microprobe and their Li contents were estimated from equations [tri 1] and [di 1] of Table 2. The Eibenstock granite constitutes one of the most evolved tin granites in the province and it contains a number of petrographically and chemically distinct subintrusions. These are designated in the legend of Fig. 13 and range in order from the least-evolved facies (EIB0) to the most evolved (EIB3), and to the aplites (A-EIB). The trioctahedral micas show a regular progression from siderophyllite to zinnwaldite in the least evolved facies to the aplites. Petrographic evidence suggests that these micas are of magmatic origin and have been formed late in the crystallization history. Late magmatic, and early metasomatic (autometasomatism) processes in these granites produced dioctahedral micas, and these show a parallel development, in the different subintrusions, from Li-poor phengites and muscovites to Li phengites(z) which nearly reach the zinnwaldite field. The Li-rich phengites in the EIB3 intrusion are hard to distinguish microscopically from the trioctahedral zinnwaldites with which they coexist. The continuous series of dioctahedral mica compositions from muscovite/phengite through Li phengite towards zinnwaldite observed in the Eibenstock granites serves as a natural example for the experimentally proved continuous solid solution between muscovite and zinnwaldite (Monier and Robert, 1986*b*).

Finally, we note that the X-axis variable [Mg–Li] is a good parameter to use as a parameter for mica composition when plotting other chemical variables (e.g. Sn, Cs) or physical properties (e.g. optical refraction). The full range of [Mg–Li] values from 6 to −4 encompasses the trioctahedral micas from phlogopite to lepidolite, and the dioctahedral micas are covered in the range from 1 to −1.4.

Acknowledgements

Our database of mica analyses is the product of many years of collaborative work. We wish to acknowledge in particular G. Friese (wet chemistry) and R. Schindler (XRF) from Berlin for their contributions in the years 1968 to 1981. R. Naumann (Potsdam) performed or supervised XRF analyses from 1982 to

1996 and also provided numerous unpublished analyses of muscovites. L. Hecht (München) and M. Geisler (Leipzig) are thanked for INAA data. D. Rhede and O. Appelt (Potsdam) assisted with electron microprobe work. U. Heitmann (Berlin) helped with statistical analysis. D. Wolf (Freiberg) granted permission to use unpublished mica analyses from the Ph.D. thesis of J. Uhlig. Finally, the senior author wishes to thank the director of the GeoForschungsZentrum Potsdam, R. Emmermann, for granting him a research stipend and office space while this study was completed. An anonymous Mineralogical Magazine referee provided constructive comments which led to an improvement of the manuscript.

This work is dedicated to the memory of Hertha Tischendorf, whose careful preparation of mica separates during several years of collaboration laid the foundation for much of the analytical work on which this paper is based. Hertha passed away in 1986 as a result of political repression in the German Democratic Republic.

References

Al-Saleh, S., Fuge, R. and Rea, W.J. (1977) The geochemistry of some biotites from the Dartmoor granite. *Proc. Ussher Soc.*, **4**, 37–48.

Bailey, S.W. (Ed.) (1984) *Micas. Reviews in Mineralogy*, **13**, Mineralogical Society of America, Chelsea.

Bargar, K.E., Beeson, M.H., Fournier, R.O. and Muffler, L.J.O. (1973) Present-day deposition of lepidolite from thermal waters in Yellowstone National Park. *Amer. Mineral.*, **58**, 901–4.

Barrière, M. and Cotton, J. (1979) Biotite and associated minerals as markers of magmatic fractionation and deuteric equilibration in granites. *Contrib. Mineral. Petrol.*, **70**, 183–92.

Basu, A.R., Rubury, E., Mehnert, H. and Tatsumoto, M. (1984) Sm-Nd, K-Ar and petrologic study of some kimberlites from Eastern United States and their implication for mantle evolution. *Contrib. Mineral. Petrol.*, **86**, 35–44.

Bea, F. (1980) Geochemistry of biotites in an assimilation process. An approach to recognition of metamorphic biotites from magmatic occurrence. *Krystalinikum*, **15**, 103–24.

Bea, F., Pereira, M.D. and Stroh, A. (1994) Mineral/leucosome trace-element partitioning in a peraluminous migmatite (a laser ablation-ICP-MS study). *Chem. Geol.*, **117**, 291–312.

Bigi, S. and Brigatti, M.F. (1994) Crystal chemistry and microstructures of plutonic biotite. *Amer. Mineral.*, **79**, 63–72.

Boettcher, A.L. and O'Neil, J.R. (1980) Stable isotope, chemical and petrographic studies of high pressure amphiboles and micas: evidence for metasomatism in the mantle source regions of alkali basalts and kimberlites. *Amer. J. Sci.*, **280-A**, 594–621.

Bokonbaev, K.D. (1976) Pecularities of metasomatic alteration of biotite in granites of the Sukhodol'sky massif (southeast Kirgizia) (Russ.). *Zap. kirg. Otd. vses. mineral. Obshch.*, **9**, 96–100.

Borodanov, V.M. (1983) Pecularities of biotite composition in granitoids associated with tungsten mineralization (Russ.). *Izvest. AN SSSR, Ser. geol.*, **7**, 76–81.

Brigatti, M.F. and Davoli, P. (1990) Crystal-structure refinements of *1M* plutonic biotites. *Amer. Mineral.*, **75**, 305–13.

Černý, P. and Burt, D.M (1984) Paragenesis, crystallochemical characteristics, and geochemical evolution of micas in granite pegmatites. In *Reviews in Mineralogy*, **13**, *Micas* (S.W. Bailey, ed.), Mineral. Soc. Amer., 257–97.

Černý, P. and Trueman, D.L. (1985) Polylithionite from rare-metal deposits of the Blachford Lake alkaline complex, N. W. T., Canada. *Amer. Mineral.*, **70**, 1127–34.

Černý, P., Rieder, M. and Povondra, P. (1970) Three polytypes of lepidolite from Czechoslovakia. *Lithos*, **3**, 319–25.

Černý, P., Stanek, J., Novák, M., Baadsgaard, H., Rieder, M., Ottolini, L., Kavalová, M. and Chapman R. (1995) Geochemical and structural evolution of micas in the Rozná and Dobrá Voda pegmatites, Czech Republic. *Mineral. Petrol.*, **55**, 177–201.

Charoy, B. and Noronha, F. (1996) Multistage growth of a rare-element, volatile-rich microgranite at Argemela (Portugal). *J. Petrol.*, **37**, 73–94.

Charoy, B., Chaussidon, M. and Noronha, F. (1995) Lithium zonation in white micas from the Argemela microgranite (central Portugal): an in-situ ion-, electron-microprobe and spectroscopic investigation. *Eur. J. Mineral.*, **7**, 335–52.

Chaudhry, M.N. and Howie, R.A. (1973) Lithium-aluminium micas from the Meldon aplite, Devonshire, England. *Mineral. Mag.*, **39**, 289-96.

Cooper, A.F., Paterson, L.A. and Reid, D.L. (1995) Lithium in carbonatites - consequence of an enriched mantle source. *Mineral. Mag.*, **59**, 401–8.

De Fino, M., La Volpe, L. and Piccarreta, G. (1983) Mafic minerals from Punta delle Pietre Nere subvolcanites (Gargano, Southern Italy): Their petrological significance. *Tscherm. Mineral. Petrogr. Mitt.*, **32**, 69–78.

De Kimpe, C.R., Miles, N., Kodama, H. and Dejou, J. (1987) Alteration of phlogopite to corrensite at Sharbot Lake, Ontario. *Clays Clay Mineral.*, **35**, 150–58.

du Bray, E.A. (1994) Compositions of micas in peraluminous granitoids of the eastern Arabian

Shield. Implications for petrogenesis and tectonic setting of highly evolved, rare-metal enriched granites. *Contrib. Mineral. Petrol.*, **116**, 381–97.

Edgar, A.D. (1992) Barium-rich phlogopite and biotite from some Quaternary alkali mafic lavas, West Eifel, Germany. *Eur. J. Mineral.*, 4, 321–30.

Edmunds, W.M., Kay, R.L.F. and McCartney, R.A. (1985) Origin of saline groundwaters in the Carnmenellis Granite (Cornwall, England): Natural processes and reaction during Hot Dry Rock reservoir circulation. *Chem. Geol.*, **49**, 287–301.

Fiala, J., Vejnar, Z. and Kucerová, D. (1976): Composition of the biotites and the coexisting biotite-hornblende pairs in granitic rocks of the Central Bohemian Pluton. *Krystalinikum*, **12**, 79–111.

Fonteilles, M. (1987) La composition chimique des micas lithinifères (et autres minéraux) des granites d'Échassières comme image de leur évolution magmatique. *Géologie de la France*, **n° 2-3**, 149–78.

Förster, H.-J. and Tischendorf, G. (1996) Compositional heterogeneity of silicic magmatic rocks from the German Variscides. *Z. geol. Wiss.*, **24**, 467–82.

Foster, M.D. (1960*a*) Interpretation of the composition of trioctahedral micas. *U.S. Geol. Survey Prof. Paper*, **354**-B, 11–49.

Foster, M.D. (1960*b*) Interpretation of the composition of lithium micas. *U.S. Geol. Survey Prof. Paper*, **354**-E, 115–47.

Ganzeeva L.V. (1973) Taeniolite of alkali metasomatic rocks from Byelorussia (Russ.). *Dokl. Ak. Nauk Byeloruss. SSR.*, **T XVII**, 560–62.

Goeman, U.E.H. (1972) Untersuchung und Berechnung einiger Biotite aus Graniten des nordwestlichen Fichtelgebirges/NE-Bayern. *Schweiz. Min. Petr. Mitt.*, **52**, 317–29.

Gottesmann, B. and Tischendorf, G. (1978) Klassifikation, Chemismus und Optik trioktaedrischer Glimmer. *Z. geol. Wiss.*, **6**, 681–708.

Gottesmann, B. and Tischendorf, G. (1980) Über Protolithionit. *Z. geol. Wiss.*, **8**, 1365–73.

Gottesmann, B., Tischendorf, G. and Förster H.-J. (1994*a*) Trioctahedral micas as indicators of the compositional evolution of Sn-Li-Rb-Cs-F granites, an example: The Eibenstock pluton (Western Erzgebirge/Germany). *16th General IMA Meeting, Pisa*, 4.-9. Sept. 1994, Abstracts, p.152.

Gottesmann, B., Tischendorf, G., Wand, U., Bielicki, K.-H., Förster, H.-J., Haase, G. and Thomas, R. (1994*b*) Die granitoiden Gesteine des Sächsischen Granulitmassivs - Petrographie, Geochemie und Altersstellung. *Hallesches Jb. Geowiss.*, **16**, 23–55.

Grew, E.S., Chernosky, J.V., Werding, G., Abraham, K., Marquez, N. and Hinthorne, J.R. (1990) Chemistry of kornerupine and associated minerals, a wet chemical, ion microprobe, and X-ray study emphasizing Li, Be, B and F contents. *J. Petrol.* **31**, 1025–70.

Grew, E.S., Hiroi, Y., Motoyoshi, Y., Kondo, Y., Jayatileke, S.J.M. and Marquez, N. (1995) Iron-rich kornerupine in sheared pegmatite from the Wanni Complex, at Homagama, Sri Lanka. *Eur. J. Mineral.*, 7, 623–36.

Harlow, G.E. (1995) Crystal chemistry of barian enrichment in micas from metasomatized inclusions in serpentinite, Motagua Fault Zone, Guatemala. *Eur. J. Mineral.*, **7**, 775–89.

Hecht, L. (1993) Die Glimmer als Indikatoren für die magmatische und postmagmatische Entwicklung der Granite des Fichtelgebirges (NE-Bayern). *Münchner Geol. Hefte*, **10**, 1–221.

Heinrich, E.Wm. (1967) Micas of the Brown Derby pegmatites, Gunnison County, Colorado. *Amer. Mineral.*, **52**, 1110–21, 1578.

Henderson, C.M.B., Martin, J.S. and Mason, R.A. (1989) Compositional relations in Li-micas from S.W.England and France: an ion- and electron-microprobe study. *Mineral. Mag.*, **53**, 427–49.

Icenhower, J. and London, D. (1997) Partitioning of fluorine and chlorine between biotite and granitic melt: experimental calibration at 200 MPa (H_2O). *Contrib. Mineral. Petrol.*, **127**, 17–29.

Jolliff, B.L., Papike, J.J. and Shearer, C.K. (1987) Fractionation trends in mica and tourmaline as indicator of pegmatite internal evolution: Bob Ingersoll pegmatite, Black Hills, South Dakota. *Geochim. Cosmochim. Acta*, **51**, 519–34.

Kramer, W. and Seifert, W. (1994) Mica-lamprophyres and related volcanics of the Erzgebirge and their metallogenic significance. In *Metallogeny of Collisional Orogens* (R. Seltmann, H. Kämpf and P. Möller, eds.) Czech Geol. Surv., Prague, 159–65.

Lapides, I.L., Kovalenko, V.I. and Koval', P.V. (1977) *The Micas of Rare-Metal Granitoids* (Russ.). Ed. Nauka, Sibirskoje Otd., Novosibirsk, 103 pp.

Livi, K.J.T. and Veblen, D.R. (1987) 'Eastonite' from Easton, Pennsylvania: A mixture of phlogopite and a new form of serpentine. *Amer. Mineral.*, **72**, 113–25.

Luecke, W. (1981) Lithium pegmatites in the Leinster granite (southeast Ireland). *Chem. Geol.*, **34**, 195–233.

Malyshonok, Yu V. (1989) Pecularities of the chemical composition of micas from the Murun Massif (Russ.). *Miner. Zhurn.*, **11/6**, 38–52.

Métais, D., Ravier, J. and Phan, K.D. (1962) Nature et composition chimique des micas de deux lamprophyres. *Bull. Soc. franc. Minér. Crist.*, **85**, 321–28.

Mokhtari, A., Wagner, C. and Velde D. (1985) Presence of late crystallizing ferriannite-rich annite in basic eruptive rocks from Morocco. *N. Jb. Miner., Mh.*, 11, 513–20.

Monier, G. and Robert, J.-L. (1986*a*) Muscovite solid solutions in the system K_2O–MgO–FeO–Al_2O_3–SiO_2–H_2O: an experimental study at 2 kbar P_{H_2O} and comparison with natural Li-free white micas. *Mineral. Mag.*, **50**, 257–66.

Monier, G. and Robert, J.-L. (1986*b*) Evolution of the miscibility gap between muscovite and biotite solid solutions with increasing lithium content: an experimental study in the system K_2O–Li_2O–MgO–FeO–Al_2O_3–SiO_2–H_2O–HF at 600°C, 2 kbar P_{H_2O}: comparison with natural lithium micas. *Mineral. Mag.*, **50**, 641–51.

Monier, G., Charoy, B., Cuney, M., Ohnenstetter, D. and Robert, J.-L. (1987) Évolution spatiale et temporelle de la composition des micas du granite albitique à topaze-lépidolite de Beauvoir. *Géol. France*, **2-3**, 179–88.

Müller, G. (1966) Die Beziehungen zwischen der chemischen Zusammensetzung, Lichtbrechung und Dichte einiger koexistierender Biotite, Muskowite und Chlorite aus granitischen Tiefengesteinen. *Contrib. Mineral. Petrol.*, **12**, 173–91.

Nash, W.P. (1993) Fluorine iron biotite from the Honeycomb Hill rhyolite, Utah: The halogen record of decompression in a silicic magma. *Amer. Mineral.*, **78**, 1031–40.

Neiva, A.M.R. (1976) The geochemistry of biotites from granites of northern Portugal with special reference to their tin content. *Mineral. Mag.*, **40**, 453–66.

Neiva, A.M.R. (1980) Chlorite and biotite from contact metamorphism of phyllite and metagraywacke by granite, aplite-pegmatite and quartz veins. *Chem. Geol.*, **19**, 49–71.

Neiva, A.M.R. (1981*a*) Geochemistry of hybrid granitoid rocks and of their biotites from central northern Portugal and their petrogenesis. *Lithos*, **14**, 149–63.

Neiva, A.M.R. (1981*b*) Geochemistry of chlorite and biotite from contact metamorphism of phyllite by granites. *Mem. Noticias, Publ. Lab. Mineral., Geol., Univ. Coimbra*, **No. 91/92**, 113–34.

Neiva, A.M.R. (1992) Geochemistry and evolution of Jales granitic system, Northern Portugal. *Chem. Erde*, **52**, 225–41.

Neiva, A.M.R. and Gomes, M.E.P. (1991) Geochemistry of the granitoid rocks and their minerals from Lixa do Alvao-Alfarela de Jales-Tourencinho (Vila Pouca de Aguiar, northern Portugal). *Chem. Geol.*, **89**, 305–27.

Němec, D. (1969) Glimmer der regionalmetamorphen Skarne Westmährens. *Tscherm. Miner. Petrogr. Mitt.*, **13**, 55–89.

Němec, D. (1983) Zinnwaldit in moldanubischen Lithium-Pegmatiten. *Chem. Erde*, **42**, 197–204.

Ottolini, L., Bottazzi, P. and Vannucci, R. (1993) Quanitification of Lithium, Beryllium, and Boron in silicates by secondary ion mass spectrometry using conventional energy filtering. *Anal. Chem.*, **65**, 1960–68.

Pechar, F. and Rykl, D. (1992) Die Vergleichung der kristallchemischen Parameter der Fe-Li-Glimmer aus den Lokalitäten Cínovec, Vysoký Kámen und des Biotits aus dem Mittelböhmischen Pluton (Czech., Germ Res.). *Ústecké Muzejní Sešity, Ústi*, **4**, 56–70.

Pomarleanu, V. and Movileanu, A. (1977/78) Contributii la geochimia biotitelor din Romania. D. S. *Inst. Geol. Geofiz., 1. Miner.-Petrol.-Geochim.*, Bucuresti, **LXV/1**, 101–20.

Rieder, M. (1970) Chemical composition and physical properties of lithium-iron micas from the Krušné hory Mts. (Erzgebirge). *Contrib. Mineral. Petrol.*, **27**, 131–58.

Rieder, M., Povondra, P. and Frýda, J. (1995) Coexisting biotite and muscovite; an example from a Moinian mica schist at Glenfinnan, Scottish Highlands. *Mineral. Petrol.*, **53**, 63–74.

Rieder, M., Haapala, I. and Povondra, P. (1996) Mineralogy of dark mica from the Wiborg rapakivi batholith, southeastern Finland. *Eur. J. Mineral.*, **8**, 593–605.

Rub M.G., Rub, A.K. and Loseva, T.I. (1971) Micas as guides for ore presence detection in granitoids (Russ.). *Izv. Ak. Nauk SSSR, Ser. geol.*, **10**, 73–85.

Rub, M.G., Pavlov, V.A., Rub, A.K., Štemprok, M., Drabek, M. and Drabkova, E. (1983) Vertical zonality of elements in Li-F granites of the Cinovec massif (CSSR) (Russ.) In *Korrelyaziya magmaticheskikh porod Chekhoslovakii i nekotorikh rayonov SSSR* (O.A. Bogatikov and A.M. Borsuk, eds.) Ed. Nauka Moskva, 108–37.

Rub M.G., Rub, A.K. and Akimov, V.M. (1986) Rare-metal bearing granites of Central Sikhote-Alin' (Russ.). *Izv. Ak. Nauk SSSR, Ser. geol.*, **7**, 33–46.

Schmidt, W. and Pietzsch, C. (1990) Iron distribution and geochemistry of pegmatitic dioctahedral $2M_1$ micas. *Chem. Erde*, **50**, 27–38.

Silva, M.M.V.G. and Neiva, A.M.R. (1990) Geochemistry of the granites and their minerals from Paredes da Beira-Penedono, northern Portugal. *Chem. Geol.*, **85**, 147–70.

Skosyreva M.V. and Vlasova E.V. (1983) First occurrence of polylithionite from rare-metal granite pegmatites (Russ.). *Dokl. Ak. Nauk SSSR*, **272/3**, 694–97.

Stone, M., Exley, C.S. and George, M.C. (1988) Compositions of trioctahedral micas in the Cornubian batholith. *Mineral. Mag.*, **52**, 175–92.

Sun Shihua (1984): The subdivision of lithium micas and their significance in the study of granitoids. In *Geology of Granites and their Metallogenetic Relations* (Xu Keqin, Tu Guangchi, eds.), Proc. of the Int. Symp., Nanjing, China, Oct. 26-30, 1982, 379–93.

Tindle, A.G. and Webb, P.C. (1990) Estimation of lithium contents in trioctahedral micas using microprobe data: application to micas from granitic rocks. *Eur. J. Mineral.*, **2**, 595–610.

Tischendorf, G., Friese, G. and Schindler, R. (1969) Die Dunkelglimmer der westerzgebirgisch-vogtländischen Granite und ihre Bedeutung als petrogenetische und metallogenetische Indikatoren. *Geologie*, **18**, 384–99, 1024–44.

Tischendorf, G., Pälchen, W., Röllig, G. and Lange, H. (1987) Formationelle Gliederung, petrographisch-geochemische Charakteristik und Genese der Granitoide der Deutschen Demokratischen Republik. *Chem. Erde*, **46**, 7–23.

Tröger, W.E. (1962) Über Protholithionit und Zinnwaldit - Ein Beitrag zur Kenntnis von Chemismus und Optik der Lithiumglimmer. *Beitr. Mineral. Petrol.*, **8**, 418–31.

Uhlig J. (1992) *Zur Mineralogie und Geochemie der Granitoid- und Greisenglimmer aus Zinnlagerstätten des Sächsischen Erzgebirges und der Mongolei.* Thesis, Bergakademie Freiberg, 129 p.

Volkov, V.N. and Gorbacheva, S.A. (1980) Variations of crystallization environment of granites in a vertical section of an intrusive body according to data on the composition of rock-forming biotite (Russ.). *Geokhimiya*, 147–53.

Wagner, C., Velde, D. and Mokhtari, A. (1987) Sector-zoned phlogopites in igneous rocks. *Contrib. Mineral. Petrol.*, **96**, 186–91.

Winchell A.N. (1942) Further studies of the lepidolite system. *Amer. Mineral.*, **27**, 114–30.

[*Manuscript received 8 January 1997:
revised 2 April 1997*]

Appendix
Sources of data on which the figures and regression equations are based

Author	Fig. 3–4 Eq. tri 1–3	Fig. 5*a* Eq. tri 4	Fig. 5b Eq. tri 5	Fig. 6*a,b* Eq. di 1–2
Foster, 1960*b*				x
Müller, 1966	x	x	x	x
Heinrich, 1967	x			
Němec, 1969	x	x		
Černý *et al.*, 1970		x	x	x
Rieder, 1970		x	x	
Rub *et al.*, 1971	x		x	
Goeman, 1972		x		
Bargar *et al.*, 1973	x	x		
Chaudhry and Howie, 1973	x	x	x	
Sun Shihua, 1974			x	
Bokonbaev, 1976	x	x		
Fiala *et al.*, 1976		x		
Neiva, 1976, 1980, 1981*b*	x		x	
Al-Saleh *et al.*, 1977	x	x		
Lapides *et al.*, 1977				x
Pomarleanu and Movileanu, 1977/78	x			
Barriére and Cotton, 1979	x	x	x	
Bea, 1980	x	x	x	
Volkov and Gorbacheva, 1980	x	x		
Luecke, 1981	x	x		x
Borodanov, 1983	x	x		
Němec, 1983	x			
Rub *et al.*, 1983	x	x	x	
Skosyreva and Vlasova, 1983	x	x		
Černý and Trueman, 1985		x		
Edmunds *et al.*, 1985	x	x		
Rub *et al.*, 1986			x	
Fonteilles, 1987	x	x	x	
Jolliff *et al.*, 1987	x		x	
Monier *et al.*, 1987	x	x	x	
Stone *et al.*, 1988	x	x	x	
Henderson *et al.*, 1989			x	x
Malyshonok, 1989	x		x	
Brigatti and Davoli, 1990	x			
Grew *et al.*, 1990	x			
Schmidt and Pietzsch, 1990				x
Silva and Neiva, 1990	x	x	x	x
Neiva and Gomes, 1991	x		x	x
Neiva, 1992				x
Pechar and Rykl, 1992	x	x	x	
Uhlig, 1992	x	x	x	x
Hecht, 1993	x		x	x
Bigi and Brigatti, 1994	x			
du Bray, 1994		x	x	x
Černý *et al.*, 1995		x	x	x
Charoy *et al.*, 1995		x	x	x
Grew *et al.*, 1995				x
Rieder *et al.*, 1995	x		x	x
Charoy and Noronha, 1996		x	x	x
Rieder *et al.*, 1996		x	x	
Authors' and Naumann's data base	x	x	x	x